

# Identification and Regulation of Plasma Membrane Sulfate Transporters in *Chlamydomonas*<sup>1[W][OA]</sup>

Wirulda Pootakham\*, David Gonzalez-Ballester, and Arthur R. Grossman

Department of Biology, Stanford University, Stanford, California 94305–5020 (W.P.); and Department of Plant Biology, The Carnegie Institution, Stanford, California 94305 (W.P., D.G.-B., A.R.G.)

*Chlamydomonas* (*Chlamydomonas reinhardtii*) exhibits several responses following exposure to sulfur (S)-deprivation conditions, including an increased efficiency of import and assimilation of the sulfate anion (SO<sub>4</sub><sup>2-</sup>). Aspects of SO<sub>4</sub><sup>2-</sup> transport during S-replete and S-depleted conditions were previously studied, although the transporters had not been functionally identified. We employed a reverse genetics approach to identify putative SO<sub>4</sub><sup>2-</sup> transporters, examine their regulation, establish their biogenesis and subcellular locations, and explore their functionality. Upon S starvation of wild-type *Chlamydomonas* cells, the accumulation of transcripts encoding the putative SO<sub>4</sub><sup>2-</sup> transporters SLT1 (for SAC1-like transporter 1), SLT2, and SULTR2 markedly increased, suggesting that these proteins function in high-affinity SO<sub>4</sub><sup>2-</sup> transport. The *Chlamydomonas sac1* and *snrk2.1* mutants (defective for acclimation to S deprivation) exhibited much less of an increase in the levels of *SLT1*, *SLT2*, and *SULTR2* transcripts and their encoded proteins in response to S deprivation compared with wild-type cells. All three transporters were localized to the plasma membrane, and their rates of turnover were significantly impacted by S availability; the turnover of SLT1 and SLT2 was proteasome dependent, while that of SULTR2 was proteasome independent. Finally, mutants identified for each of the S-deprivation-responsive transporters were used to establish their critical role in the transport of SO<sub>4</sub><sup>2-</sup> into S-deprived cells.

Sulfur (S) is an essential element for all organisms and is present in proteins, lipids, carbohydrates, and several metabolites. Sulfate (SO<sub>4</sub><sup>2-</sup>) is the preferred S source for most organisms. In photosynthetic organisms, the reductive assimilation of SO<sub>4</sub><sup>2-</sup> occurs in plastids, which means that this ion must traverse both the plasma membrane and the plastid envelope prior to reduction and incorporation into organic molecules. SO<sub>4</sub><sup>2-</sup> is relatively inert and must be activated by the enzyme ATP sulfurylase before being reduced to sulfide and incorporated into the amino acids Cys and Met (Leustek et al., 2000), which can be used for the synthesis of proteins or converted into other metabolites, including glutathione and dimethyl sulfide.

Much of the SO<sub>4</sub><sup>2-</sup> in the soil is not readily available to plants or microbes. The SO<sub>4</sub><sup>2-</sup> anion can be adsorbed onto the surface of the soil particles, and a large proportion may be covalently bonded to organic molecules in the form of SO<sub>4</sub><sup>2-</sup> esters and sulfonates. When experiencing low SO<sub>4</sub><sup>2-</sup> availability, the unicellular, soil-dwelling alga *Chlamydomonas*

*reinhardtii* exhibits a suite of responses that include the synthesis of extracellular arylsulfatases (ARS), elevated SO<sub>4</sub><sup>2-</sup> transport activity, and an increase in the levels of transcripts encoding ATP sulfurylase and other enzymes associated with S assimilation. Many of these responses allow the alga to more efficiently scavenge and assimilate available SO<sub>4</sub><sup>2-</sup> in the environment (Davies and Grossman, 1998; Grossman and Takahashi, 2001; Zhang et al., 2004; Gonzalez-Ballester et al., 2008, 2010; Shibagaki and Grossman, 2008).

Specific polypeptides involved in regulating *Chlamydomonas* S-deprivation responses have been identified. The SAC1 (for sulfur acclimation 1) protein is required for many S-limitation-induced responses. *Chlamydomonas* mutants with lesions in the *SAC1* gene exhibit abnormal SO<sub>4</sub><sup>2-</sup> uptake, are unable to synthesize extracellular ARS, and show little increase in many S-deprivation-responsive transcripts, including those encoding ARS, ATP sulfurylase, Ser acetyltransferase, and the ferredoxin-dependent sulfite reductase. Furthermore, *sac1* mutants cannot suppress photosynthetic electron transport activity and rapidly die when placed in S-deficient medium in the light. Even though the *SAC1* gene encodes a protein similar to anion transporters from a number of different organisms, including the Na<sup>+</sup>/SO<sub>4</sub><sup>2-</sup> transporter from mammals, the phenotypes of *sac1* mutants strongly suggest that SAC1 functions in regulating cellular responses to S deprivation (Davies et al., 1996). A second polypeptide that plays a central role in the acclimation of *Chlamydomonas* to S deprivation is SNRK2.1, a member of the SNF1-related protein kinase

<sup>1</sup> This work was supported by the National Science Foundation (grant nos. MCB0235878 and MCB0824469 to A.R.G.) and by a Marie Curie award (grant no. MOIF-CT-2006-40208-APOSD to D.G.-B.).

\* Corresponding author; e-mail [wirulda@gmail.com](mailto:wirulda@gmail.com).

The author responsible for distribution of materials integral to the findings presented in this article in accordance with the policy described in the Instructions for Authors ([www.plantphysiol.org](http://www.plantphysiol.org)) is: Arthur R. Grossman ([arthurg@stanford.edu](mailto:arthurg@stanford.edu)).

[W] The online version of this article contains Web-only data.

[OA] Open Access articles can be viewed online without a subscription.

[www.plantphysiol.org/cgi/doi/10.1104/pp.110.157875](http://www.plantphysiol.org/cgi/doi/10.1104/pp.110.157875)

2 family. Like SAC1, SNRK2.1 is required for most responses associated with the acclimation of *Chlamydomonas* to S deprivation. A *snrk2.1* mutant (initially designated *ars11*) is defective for the expression of several S-responsive genes, and the mutant bleaches and dies more rapidly than wild-type cells during S starvation; the responses of *snrk2.1* to S deprivation are generally more severe than those of the *sac1* mutant (Gonzalez-Ballester et al., 2008).

Increased  $\text{SO}_4^{2-}$  uptake in response to S limitation has been extensively documented for prokaryotic and eukaryotic organisms, including *Escherichia coli*, *Neurospora crassa*, *Saccharomyces cerevisiae*, and *Arabidopsis* (*Arabidopsis thaliana*; Breton and Surdin-Kerjan, 1977; Ketter and Marzluf, 1988; Shibagaki et al., 2002; Gyaneshwar et al., 2005). In prokaryotic organisms,  $\text{SO}_4^{2-}$  is often transported into the cell by a single transport system, whereas eukaryotes often have multiple  $\text{SO}_4^{2-}$  transporters. In *S. cerevisiae* and *Arabidopsis*, there are both high- and low-affinity  $\text{SO}_4^{2-}$  transporters (Breton and Surdin-Kerjan, 1977; Leustek et al., 2000). Increased accumulation of transcripts encoding  $\text{SO}_4^{2-}$  transporters upon S starvation has also been noted for *S. cerevisiae*, *N. crassa*, and *Arabidopsis* (Ketter and Marzluf, 1988; Cherest et al., 1997; Yoshimoto et al., 2002).

*Arabidopsis* has 12 putative  $\text{SO}_4^{2-}$  transporters that have been classified into four groups. The AtSULTR1 group represents high-affinity transporters responsible for the initial uptake of  $\text{SO}_4^{2-}$  into root cells, while AtSULTR2;1, AtSULTR2;2, and AtSULTR3;5 are low-affinity transporters likely to play important roles in the translocation of  $\text{SO}_4^{2-}$  from roots to leaves (Takahashi et al., 2000; Hawkesford, 2003; Kataoka et al., 2004a). Furthermore, two isoforms of the AtSULTR4 group have been localized to the tonoplast and facilitate  $\text{SO}_4^{2-}$  efflux from vacuoles (Kataoka et al., 2004b). The plant-associated  $\text{H}^+/\text{SO}_4^{2-}$  cotransporters usually contain 12 transmembrane domains followed by a linking region that connects to a C-terminal STAS (for  $\text{SO}_4^{2-}$  transporter and anti-sigma factor antagonist) domain. There is significant interest in the function of the STAS domain, since lesions in this domain can lead to serious human diseases (Everett and Green, 1999). While the precise function of the STAS domain is not clear, it is required for the activity and proper assembly of the  $\text{SO}_4^{2-}$  transporters (Shibagaki and Grossman, 2004, 2006; Rouached et al., 2005) and may help regulate interactions of the transporter with partner proteins that function downstream in the S assimilation pathway (Shibagaki and Grossman, 2010).

Features of  $\text{SO}_4^{2-}$  transport in *Chlamydomonas* during S-replete and S-depleted conditions have been reported, although there has been little molecular characterization of the genes and polypeptides encoding the putative  $\text{SO}_4^{2-}$  transporters. Initial studies demonstrated that both the  $V_{\max}$  and the substrate concentration at which  $\text{SO}_4^{2-}$  transport is at half-maximum velocity ( $K_{1/2}$ ) were altered in S-depleted

cells. The  $V_{\max}$  increased approximately 10-fold and the  $K_{1/2}$  decreased roughly 7-fold. The enhancement of  $\text{SO}_4^{2-}$  transport upon S deprivation is prevented by cycloheximide (CHX) but not by chloramphenicol, demonstrating that protein synthesis on 80S cytoplasmic ribosomes is required for the synthesis of the high-affinity transport systems (Yildiz et al., 1994).

Analysis of the *Chlamydomonas* genome sequence has led to the identification of several genes encoding proteins with high sequence similarity to known  $\text{SO}_4^{2-}$  transporters. Three of the putative  $\text{SO}_4^{2-}$  transporters (SULTR1 to SULTR3) are in the  $\text{H}^+/\text{SO}_4^{2-}$  family (characteristic of vascular plants), while another three (SLT1 to SLT3; for SAC1-like transporter) are in the  $\text{Na}^+/\text{SO}_4^{2-}$  transporter family that is present in bacteria, nonvascular plants, and mammals; these transporters have not been identified in vascular plants. Another SULTR-type transporter, originally designated SULTR4, was recently shown to encode a functional molybdate transporter, and the gene has been renamed *MOT1* (Tejada-Jiménez et al., 2007). Transcripts from some of the transporter genes increase significantly during S deprivation; increased accumulation of *SLT1* and *SULTR2* transcripts during S starvation was previously reported (Gonzalez-Ballester et al., 2008). *Chlamydomonas* also possesses  $\text{SO}_4^{2-}$  permeases (SulP1 and SulP2) that resemble the permeases of bacteria (Laudenbach and Grossman, 1991; Chen et al., 2003; Lindberg and Melis, 2008). These transport proteins have been localized to the chloroplast envelope and function in the transport of  $\text{SO}_4^{2-}$  from the cytosol into chloroplasts, where reductive assimilation of the anion occurs.

Here, we identify, localize, and examine the regulation of *Chlamydomonas*  $\text{SO}_4^{2-}$  transporters. We define the kinetics of accumulation of both the RNA encoding the transporters and the transporter polypeptides following the imposition of S deprivation and monitor their decay after  $\text{SO}_4^{2-}$  is added back to starved cells. We also evaluate the impact of the regulatory elements SAC1 and SNRK2.1 on the accumulation of *SULTR* and *SLT* transcripts in S-replete and S-depleted cells and show that the proteasome is involved in the turnover of SLT but not SULTR transporters. Finally, various methods were used to localize the different transporters to specific cellular membranes and to identify and characterize mutants that were specifically defective for the function of the individual transporter polypeptides. These analyses provide a comprehensive view of the function, biogenesis, and regulation of the S-responsive  $\text{SO}_4^{2-}$  transporters in *Chlamydomonas*.

## RESULTS

### *Chlamydomonas* $\text{SO}_4^{2-}$ Transporter Genes and Proteins

Previous work identified full-length cDNA clones encoding the *Arabidopsis* and *Stylosanthes hamata*

$\text{SO}_4^{2-}$  transporters. These genes were characterized and used to identify potential  $\text{SO}_4^{2-}$  transporters from other species (Takahashi et al., 1997). Similarly, analysis of the entire *Chlamydomonas* genome sequence (Merchant et al., 2007) allowed us to identify genes encoding putative  $\text{SO}_4^{2-}$  transporters in this alga. Six candidate genes (*SULTR1* to *SULTR3* and *SLT1* to *SLT3*) were identified based on homologies to plant, animal, and bacterial  $\text{SO}_4^{2-}$  transporters. The deduced amino acid sequences of *SULTR1* and *SULTR2* are highly similar (60%) to the  $\text{H}^+/\text{SO}_4^{2-}$  cotransporters (SLC26 family) from vascular plants, including those of *Arabidopsis* and *S. hamata* (Supplemental Fig. S1A), although both of the *Chlamydomonas* transporter proteins have an insertion of 17 amino acids starting at amino acid 199 of *SULTR1*. The deduced amino acid sequence of *SULTR3* is more similar to  $\text{SO}_4^{2-}$  transporters from bacteria. *SULTR1* and *SULTR2* of *Chlamydomonas* are most similar to *Arabidopsis* At*SULTR1;2* and At*SULTR4* (Supplemental Fig. S1A). The C-terminal STAS domain of *SULTR* transporters (Supplemental Fig. S1A, red bar) is present on various anion transporters and extends into the cytoplasm of the cell.

In contrast to the *SULTR*-type transporters, the deduced amino acid sequences of *SLT1*, *SLT2*, and *SLT3* of *Chlamydomonas* exhibit strong sequence similarity to  $\text{Na}^+/\text{SO}_4^{2-}$  transporters (SLC13 family). All three members of the *SLT* family in *Chlamydomonas* have 10 to 12 predicted transmembrane domains and an intracellular loop containing a TrkA-C domain (Supplemental Fig. S1B, orange bar). While the precise function of the TrkA-C domain is not known, it may be involved in the regulation of  $\text{SO}_4^{2-}$  transporter activity, potentially through interactions with partner proteins. The similarity among the *Chlamydomonas* *SLTs* and between the *SLTs* and the putative  $\text{SO}_4^{2-}$  transporter of the moss *Physcomitrella patens* is shown in Supplemental Figure S1B.

#### Induction of $\text{SO}_4^{2-}$ Transport and Accumulation of *SULTR2*, *SLT1*, and *SLT2* Transcripts during S Deprivation

When organisms are deprived of S, they often exhibit increases in their affinity for  $\text{SO}_4^{2-}$  (decrease in the  $K_{1/2}$ ) and in the maximal rate of  $\text{SO}_4^{2-}$  transport (elevated  $V_{\text{max}}$ ). As shown in Figure 1, the maximal rate of  $\text{SO}_4^{2-}$  transport into wild-type *Chlamydomonas* cells (strain 21gr) increases approximately 13-fold after 24 h of S deprivation. To identify those transporters likely to be responsible for the change in kinetics of  $\text{SO}_4^{2-}$  transport by cells acclimated to S deprivation, we monitored changes in the abundance of transcripts encoding the putative  $\text{SO}_4^{2-}$  transporters of *Chlamydomonas* by real-time quantitative PCR (RT-qPCR). RNAs were isolated from wild-type cells placed in medium devoid of S, nitrogen (N), or phosphorus (P) for 12 h. The elevated levels (note the log scale) for transcripts from *ARS2* (encoding an

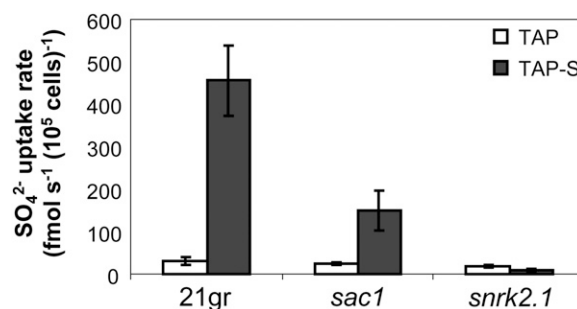


**Figure 1.**  $\text{SO}_4^{2-}$  uptake in wild-type *Chlamydomonas* cells (21gr) and the *sac1* and *snrk2.1* mutant strains. Uptake rates were determined at  $250 \mu\text{M}$   $\text{SO}_4^{2-}$  (specific activity,  $330 \text{ Ci mol}^{-1}$ ). The initial  $\text{SO}_4^{2-}$  uptake rate was calculated from the slope of the line defining the transport of  $\text{SO}_4^{2-}$  into cells as a function of time. The values are averages of three experiments with a single biological replicate, although similar results were obtained in independent experiments, and error bars represent 1 SD.

extracellular ARS) during S deprivation, from *PHOX* (encoding an alkaline phosphatase) during P deprivation, and from *NIT1* (encoding a nitrate reductase) during N deprivation (Fig. 2) suggest that the cells were responding normally to each nutrient starvation. Transcripts encoding the  $\text{SO}_4^{2-}$  transporters showed remarkable changes in abundance when the cells were starved for S but not when starved for P or N (Fig. 2). *SULTR2* and *SLT2* transcript levels increased by more than 100-fold, while the level of the *SLT1* transcript exhibited an increase of approximately 1,000-fold after 12 h of S deprivation. In contrast, *SULTR1* and *SLT3* transcript levels decreased roughly 1,000- and 10-fold, respectively, specifically during S deprivation, while the abundance of the *SULTR3* transcript exhibited little change (Fig. 2). The accumulation of *SULTR2*, *SLT1*, and *SLT2* transcripts following the imposition of S deprivation suggests that these three genes may encode the dominant, potentially high-affinity  $\text{SO}_4^{2-}$  transporters, while the decrease in *SULTR1* and *SLT3* transcript levels suggests that they may encode low-affinity  $\text{SO}_4^{2-}$  transporters (not needed in an S-limited environment).

The induction of  $\text{SO}_4^{2-}$  transport activity observed in wild-type *Chlamydomonas* cells during S limitation is reduced in the *sac1* mutant and completely abolished in the *snrk2.1* mutant (Fig. 1). To understand the relationship between transporter activity and the levels of transcripts encoding the different transporters, we quantified  $\text{SO}_4^{2-}$  transporter transcripts in wild-type and mutant strains. While the level of the *ARS2* transcript increased approximately 3 orders of magnitude in wild-type cells (21gr) within 2 h of S deprivation (Fig. 3A), the *sac1* and *snrk2.1* mutants showed marked reductions in the increase in *ARS2* mRNA abundance relative to wild-type cells (Fig. 3, B and C, respectively). Furthermore, the elevation (*SULTR2*, *SLT1*, *SLT2*) and depression (*SULTR1*, *SLT3*) of levels of transcripts encoding the various putative  $\text{SO}_4^{2-}$  transporters following

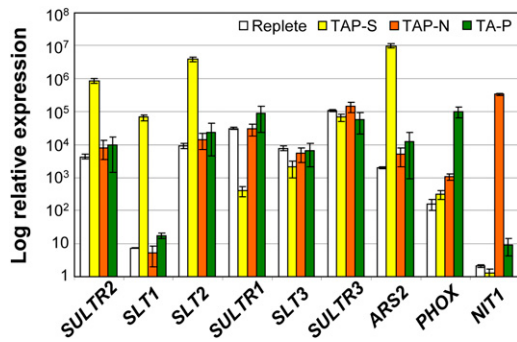


**Figure 2.** RT-qPCR analysis of transcript accumulation. Levels of *SULTR2*, *SLT1*, *SLT2*, *SULTR1*, *SLT3*, *SULTR3*, *ARS2*, *PHOX*, and *NIT1* transcripts were measured in cells deprived of S, N, or P (samples were collected 12 h after transferring cells from nutrient-replete medium to medium devoid of S, N, or P). Levels of individual transcripts are represented as relative abundance with respect to the housekeeping control gene (*CBLP*).

S deprivation were generally not nearly as marked in *sac1*, and especially in *snrk2.1*, relative to wild-type cells. The levels of accumulation of the *SULTR2*, *SLT1*, and *SLT2* polypeptides were consistent with their transcript abundances during S starvation (Supplemental Fig. S2).

Interestingly, some transcripts encoding transporters were still elevated in the mutants following S deprivation; the most notable examples are the *SLT1* transcript in the *sac1* mutant and the *SULTR2* transcript in the *snrk2.1* mutant (Fig. 3, B and C); the *SULTR2* transcript is also elevated to some extent under S-replete conditions in the *sac1* mutant. Furthermore, while the *SULTR2* transcript still increases significantly in *snrk2.1*, the absolute level of the transcript is much lower in the mutant than in the wild-type strain (2–3 orders of magnitude) under both S-replete and S-deprivation conditions. Also, the increase in the *SLT1* transcript in the *sac1* mutant is only observed after 24 h of S deprivation (it is observed 2 h after wild-type cells are exposed to S deprivation). The *SLT1* transcript in the *snrk2.1* strain is essentially not detected under S-replete or S-deprivation conditions. Finally, while the level of the *SULTR1* transcript markedly declines in wild-type cells, its decline is diminished in the *sac1* mutant, and it actually increases by 5- to 10-fold in the *snrk2.1* strain. The *SULTR3* transcript, which also decreases to some extent in the wild-type strain during S deprivation, may increase slightly in the *snrk2.1* mutant (Fig. 3, compare A and C). These results suggest that there are some complex relationships linking the mutant phenotypes to transcript levels, although regulation in the mutant strains is aberrant for essentially all transporter transcripts that were examined; we conclude that the *SAC1* and *SNRK2.1* regulators are required for both increases and decreases in transcript abundance that are observed following the transfer of *Chlamydomonas* cells to S-deprivation conditions. Furthermore, *SNRK2.1*

appears to be important for maintaining moderate levels of *SLT1* and *SULTR2* transcripts when the cells are growing in nutrient-replete medium. Finally, some of the transcripts encoding transporters that normally sharply decline in wild-type cells during S deprivation can become elevated in the mutant strains (*SULTR1* in the *snrk2.1* mutant). These findings suggest that there may be both direct and indirect consequences of elimination of the *SAC1* and/or *SNRK2.1* regulatory proteins during S deprivation on the level of transporter transcripts; the increase in the *SULTR3* transcript in *snrk2.1* might reflect the inability of the strain to suppress expression of the *SULTR3* gene, which might be the result of a compensatory effect elicited in cells severely compromised in their ability to scavenge S from external and probably internal sources.

**SULTR2, SLT1, and SLT2 Protein Levels**

We analyzed wild-type cells for levels of *SULTR2*, *SLT1*, and *SLT2* transcripts and polypeptides, both

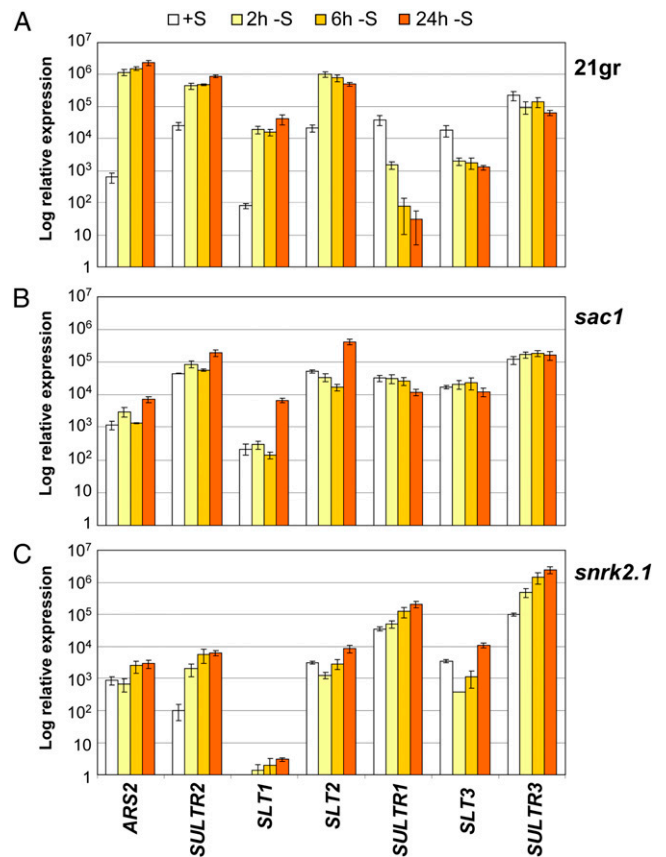


**Figure 3.** Changes in transcript abundance for the various  $SO_4^{2-}$  transporters following imposition of S deprivation. Levels of transcripts encoding *ARS2*, *SULTR2*, *SLT1*, *SLT2*, *SULTR1*, *SLT3*, and *SULTR3* were measured by RT-qPCR for wild-type cells (A) and the *sac1* (B) and *snrk2.1* (C) mutants. RNA samples were isolated from cells 0, 2, 6, and 24 h after they were transferred from TAP to TAP–S medium. The increase in *ARS2* transcript abundance was used as a positive control to demonstrate proper S-starvation responses in wild-type cells.

before and during S deprivation and following the addition of  $\text{SO}_4^{2-}$  back to starved cells. Figure 4A shows the levels of these transcripts in cells collected at various times from 1 to 32 h after removal of S from the medium and at 1, 2, 4, and 8 h after the addition of  $\text{SO}_4^{2-}$  to cells that had experienced 24 h of S starvation. The same samples that were used to quantify transcript abundance by RT-qPCR were also used for microsomal membrane preparations to monitor the levels of the transporter proteins by western-blot analyses, as shown in Figure 4B.

As presented in Figure 4A, levels of *SULTR2*, *SLT1*, and *SLT2* transcripts are high after 1 h of S deprivation and remain at approximately the same level after 24 h

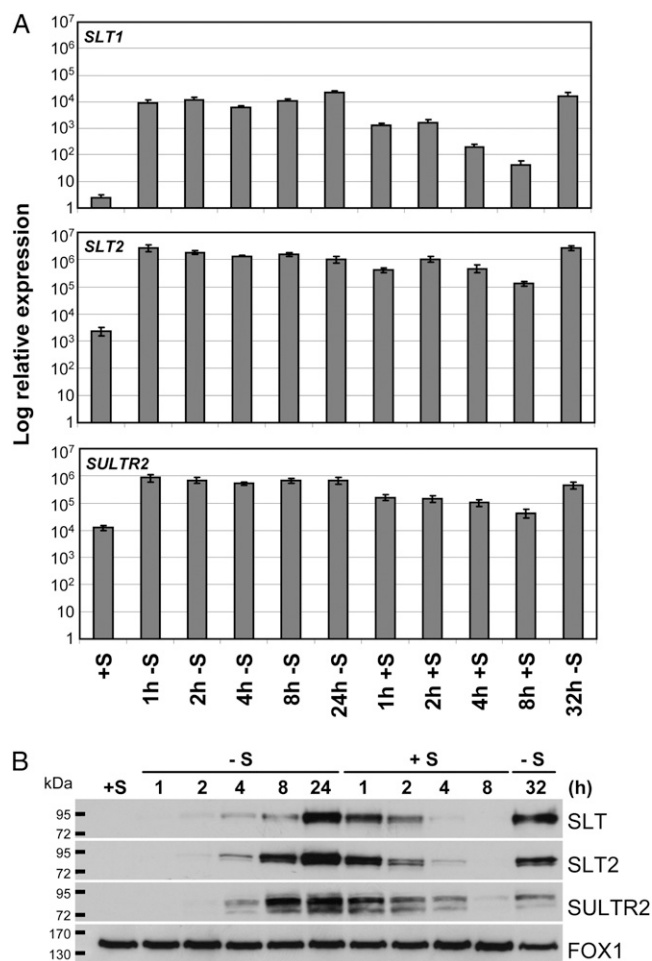


**Figure 4.** Accumulation of *SULTR2*, *SLT1*, and *SLT2* transcripts and proteins and their decay following the addition of  $\text{SO}_4^{2-}$  to S-deprived cells. Time course of accumulation of *SULTR2*, *SLT1*, and *SLT2* mRNAs (A) and polypeptides (B) upon transfer of cells from S-replete to TAP-S medium is shown. After 24 h in TAP-S, 1 mM  $\text{MgSO}_4$  was added to starved culture. Samples were taken at 1, 2, 4, 8, 24, and 32 h after the starvation (from +S to -S) and 1, 2, 4, and 8 h after the addition of  $\text{SO}_4^{2-}$  back to cultures that had been S starved for 24 h. RNA and protein isolations are described in "Materials and Methods." A ferroxidase, FOX1, served as a loading control (accumulation of FOX1 is S independent).

of S deprivation. However, these mRNAs decline at different rates following the addition of  $\text{SO}_4^{2-}$  to the medium. The *SLT1* transcript declined most rapidly, although none of the transcripts dropped to the +S levels, even at 8 h following the readdition of  $\text{SO}_4^{2-}$  to the medium.

For monitoring transporter protein abundance, polyclonal antibodies were raised against a peptide unique to SLT2 (Supplemental Fig. S1B, magenta bar), a peptide unique for SULTR2 (Supplemental Fig. S1A, blue bar), and a peptide present in both SLT1 and SLT2 (SLT "general" antibodies; Supplemental Fig. S1B, green bar; see "Materials and Methods"). The SLT general antibodies (SLT in Fig. 4B) detected a specific band of approximately 95 kD, which corresponds to the predicted molecular mass of SLT1 and SLT2 (93 and 96 kD, respectively). The specific SULTR2 antibodies recognized a polypeptide of approximately 80 kD, which corresponds to the predicted molecular mass of SULTR2 (approximately 84 kD). Generally, all of the transporter polypeptides appear to migrate as doublets (the most well-resolved doublet is for SULTR2), which could be a consequence of protein modification, proteolytic cleavage of a short N- or C-terminal region, and/or the recognition of more than one polypeptide by the antibodies (although the two proteins would have to show the same kinetic changes with respect to the S status of the medium). The marked, rapid accumulation of the transcript for the SLT and SULTR2 transporters (after 1 h of S deprivation; Fig. 4A) is followed by a dramatic increase in the levels of the transporter polypeptides, which is first detected 2 h after the initiation of S deprivation (Fig. 4B). Following administration of  $\text{SO}_4^{2-}$  to S-starved cultures, the levels of SULTR2, SLT2, and probably SLT1 (detected by the general SLT antibody and confirmed by analysis of transporter polypeptides in strains defective for specific  $\text{SO}_4^{2-}$  transporters; see Fig. 9 below) polypeptides declined and became barely detectable 8 h after the  $\text{SO}_4^{2-}$  content of the medium had been replenished (Fig. 4B). We also observed some decline in polypeptide levels at 32 h relative to 24 h of S deprivation, although the decline was much less severe than in cultures administered S.

#### Turnover of SULTR2, SLT1, and SLT2 Polypeptides

We analyzed whether the decrease in abundance of the  $\text{SO}_4^{2-}$  transporters following the addition of  $\text{SO}_4^{2-}$  was a consequence of enhanced degradation. Cells were placed in medium devoid of S for 10 h to allow the accumulation of  $\text{SO}_4^{2-}$  transporter polypeptides prior to the administration of CHX, an inhibitor of protein synthesis on 80S ribosomes, with or without the addition of 1 mM  $\text{SO}_4^{2-}$ . The concentration of CHX used in these experiments was previously shown to specifically block cytoplasmic protein synthesis (Kawazoe et al., 2000); it also completely blocked accumulation of the  $\text{SO}_4^{2-}$  transporter proteins in cells transferred to medium lacking S (Supplemental Fig.

S3). The levels of the  $\text{SO}_4^{2-}$  transporters were monitored 20, 60, and 240 min following the addition of the inhibitor and/or  $\text{SO}_4^{2-}$  to the cultures. As expected, the  $\text{SO}_4^{2-}$  transporters accumulated after 10 h of S starvation (Fig. 5A, lane 2). Interestingly, these polypeptides were turned over significantly more rapidly in cultures that received  $\text{SO}_4^{2-}$  along with CHX (Fig. 5A, lanes 10–12) compared with cultures that were only administered CHX but remained S starved (Fig. 5A, lanes 4–6). The band intensity was quantified, normalized to the level of the FOX1 protein, and the half-life of each polypeptide was derived by fitting the values to the decaying exponential equation. These results indicate that administration of  $\text{SO}_4^{2-}$  enhances degradation of the SULTR2, SLT1, and SLT2 polypeptides, although the kinetics of the turnover varies among the transporters. Since the SLT general antibodies recognize both SLT1 and SLT2 polypeptides, the half-life estimated from the signals detected with these antibodies reflects the turnover rate of both SLT proteins. Interestingly, when  $\text{SO}_4^{2-}$  was added back to the

cultures, the addition of CHX made little difference to the kinetics of the loss of SLT and SULTR2 polypeptides (Fig. 5A, compare lanes 7–9 with 10–12), raising the possibility that the addition of  $\text{SO}_4^{2-}$  to starved cultures both rapidly blocked the synthesis of these proteins (which in part also declines because of transcript degradation) and stimulated their degradation.

To determine whether the proteasome was involved in degradation of the  $\text{SO}_4^{2-}$  transporters, we performed a similar experiment in which cells were S starved for 10 h prior to the addition of CHX and  $\text{SO}_4^{2-}$  to the cultures in the presence and absence of the proteasome inhibitor MG132; samples were collected 30, 90, and 240 min following the addition of the inhibitors plus  $\text{SO}_4^{2-}$ . Figure 5B shows that degradation of SLT1 and SLT2 polypeptides was completely blocked by MG132, suggesting that proteasome activity is required for the turnover of these proteins. Intriguingly, SULTR2 turnover was not affected when proteasome function was inhibited (repeated on three separate samples with similar results), suggesting that there are different mechanisms for eliminating the transporter proteins once S becomes sufficient in the environment.

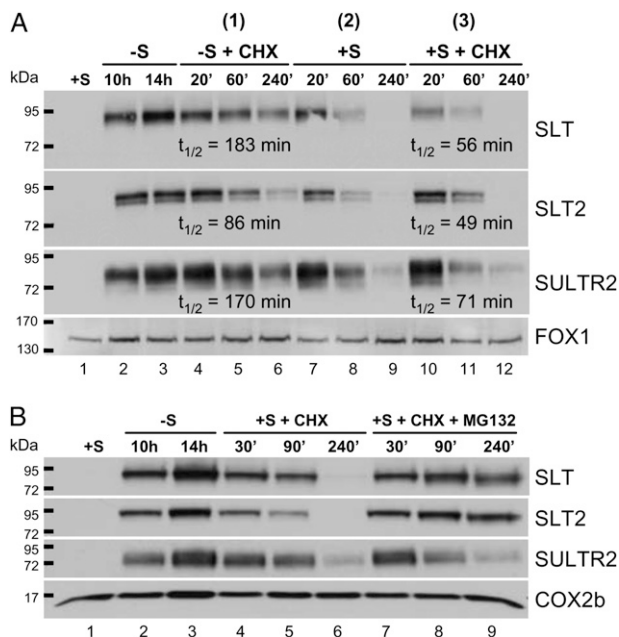


**Figure 5.** Determination of half-lives of SULTR2, SLT1, and SLT2 proteins and the role of the proteasome in degradation. **A**, *Chlamydomonas* cells were grown in TAP and transferred to TAP–S. After 10 h of starvation, the culture was split into three aliquots: CHX was added to aliquots 1 and 3, and 1 mM  $\text{SO}_4^{2-}$  was added to aliquots 2 and 3. Samples were taken prior to starvation (lane 1), after 10 and 14 h of starvation (lanes 2 and 3, respectively), and 20, 60, and 240 min after the addition of CHX (lanes 4–6),  $\text{SO}_4^{2-}$  (lanes 7–9), and  $\text{SO}_4^{2-}$  + CHX (lanes 10–12). **B**, Identical cultures were used for this analysis, except that the cells starved for S for 10 h were administered  $\text{SO}_4^{2-}$  + CHX (lanes 4–6) or  $\text{SO}_4^{2-}$  + CHX + MG132 (lanes 7–9). The experiment was repeated three independent times, yielding essentially identical results, with representative data shown. The signal strength of each band was quantified by ImageJ software (Abramoff et al., 2004) and fitted to the exponential decay equation to obtain half-lives ( $t_{1/2}$ ). A cytochrome c oxidase, COX2b, served as a loading control.

### Transporter Localization

To localize the  $\text{SO}_4^{2-}$  transporters, total membranes were prepared from S-starved cells and separated by a two-phase aqueous polymer system into a plasma membrane (polyethylene glycol) fraction and a fraction containing the rest of the cellular membranes. The polypeptides from the plasma membrane and “other membrane” (non-plasma membrane) fractions were resolved by SDS-PAGE, and immunoblot analyses were performed using antibodies to proteins of known localization. As shown in Figure 6A, the plasma membrane fraction was largely free of contamination from the thylakoid membrane and chloroplast envelope, based on the distribution of CRD1 (Allen et al., 2008), and from the mitochondrial membrane, based on the distribution of COX2b (Page et al., 2009). As expected, two plasma membrane markers,  $\text{H}^+$ -ATPase (Norling et al., 1996) and FOX1 ferroxidase (Herbik et al., 2002), partitioned preferentially to the phase with the plasma membrane (polyethylene glycol). SLT2 and SULTR2 were detected almost exclusively in the plasma membrane fraction; however, a weak signal with the general SLT antibodies was also observed in the non-plasma membrane fraction. This latter partitioning pattern is similar to that of a tonoplast V-ATPase. In order to clearly establish whether or not these  $\text{SO}_4^{2-}$  transporters are localized to the plasma membrane, proteins from the polyethylene glycol phase were separated on a 15% to 45% Suc gradient (Fig. 6B). While the tonoplast V-ATPase was mainly in fractions 7 to 9, SLT1, SLT2, and SULTR2 migrated to the bottom of the gradient and were clearly localized with the plasma membrane marker proteins FOX1 ferroxidase and the  $\text{H}^+$ -ATPase (fractions 1–3).

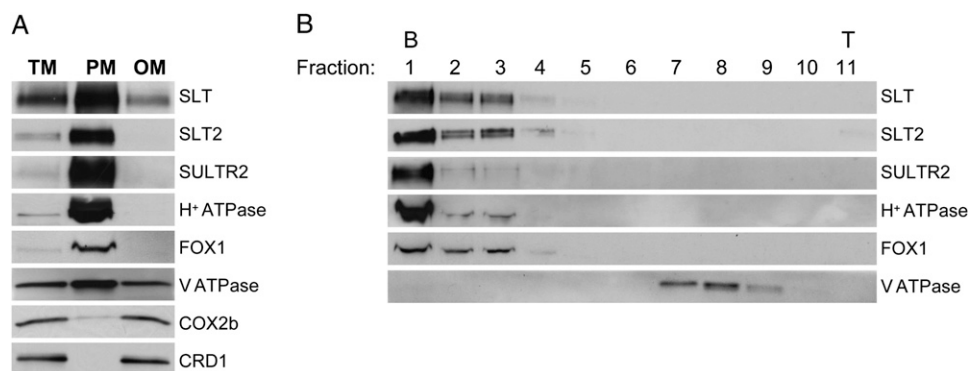


**Figure 6.** Localization of the *Chlamydomonas* SLT1, SLT2, and SULTR2 transport proteins. A, *Chlamydomonas* strain D66 was grown in TAP medium to midlogarithmic phase and then grown in TAP–S for an additional 24 h. Total membranes (TM) were isolated and partitioned into plasma membrane fraction (polyethylene glycol fraction; PM) and a fraction containing all other membranes (dextran fraction; OM). A total of 20  $\mu$ g of protein from each fraction was resolved by SDS-PAGE and transferred to a polyvinylidene difluoride membrane for immunoblot analyses using antibodies against SLT, SLT2, SULTR2, plasma membrane H<sup>+</sup>-ATPase, FOX1 ferroxidase (plasma membrane), CRD1 (thylakoid membrane and chloroplast envelope), COX2b (mitochondrial inner membrane), and V-ATPase (tonoplast). B, To separate the plasma membrane from the tonoplast, 600  $\mu$ g of protein from the polyethylene glycol phase was loaded onto a 15% to 45% Suc gradient and separated into 11 fractions of equal volume (fraction 1 is at the bottom [B] of the gradient and fraction 11 is at the top [T] of the gradient). The proteins of each fraction were resolved by SDS-PAGE and transferred to a polyvinylidene difluoride membrane for immunoblotting, as described in “Materials and Methods.”

### Expression in Heterologous Systems

To demonstrate that *SULTR2*, *SLT1*, and *SLT2* encode functional  $\text{SO}_4^{2-}$  transporters, their cDNA clones were used to functionally complement the *S. cerevisiae* (yeast) uracil auxotrophy strain CP60-1C, which harbors mutations in the *SUL1* and *SUL2*  $\text{SO}_4^{2-}$  transporter genes. CP60-1C grows very slowly on medium containing 100  $\mu\text{M}$   $\text{SO}_4^{2-}$  (or less) as a sole S source (Cherest et al., 1997). Supplemental Table S1 shows that expression of *Chlamydomonas* *SULTR2*, *SLT1*, and *SLT2* did not rescue the slow-growth phenotype of the CP60-1C strain in liquid medium containing 100  $\mu\text{M}$   $\text{SO}_4^{2-}$  as a sole S source; the same growth rate was observed for yeast cells carrying the vector alone and those carrying plasmids with *Chlamydomonas*  $\text{SO}_4^{2-}$  transporter genes. Both the GFP-tagged and untagged forms of transporters yielded the same results (failure to complement the yeast mutant). In contrast, CP60-1C cells transformed with *Arabidopsis* *SULTR1;2* cDNA exhibited a significantly shorter doubling time. *AtSULTR1;2* has previously been shown to rescue the yeast  $\text{SO}_4^{2-}$  transporter mutant (Shibagaki et al., 2002).

### Generation of an Insertional Mutant Library

Our inability to confirm the functionality of the putative  $\text{SO}_4^{2-}$  transporters using the heterologous system prompted us to screen for *Chlamydomonas* strains bearing mutations in those transporter genes. Insertional mutagenesis has been widely used in *Chlamydomonas* to generate mutant strains affecting various biological processes. To obtain mutants with insertions in the putative  $\text{SO}_4^{2-}$  transporter genes, we

generated a library containing approximately 52,000 insertional mutants using D66 as the parental strain. Cells were transformed with a 1.7-kb PCR fragment containing the *AphVIII* gene, which confers resistance to the antibiotic paromomycin, and transformants were plated on selective medium. The steps in the construction of the mutant library are described in “Materials and Methods.” Genomic DNA isolated from transformants was screened by PCR to identify specific gene disruptions. Mutants with an insertion in the  $\text{SO}_4^{2-}$  transporter genes were identified by PCR using a target gene-specific primer and a primer specific to the inserted DNA (Supplemental Table S2 shows the list of primer pairs that were used). PCR products were sequenced to confirm that the disruption was in the targeted transporter gene. The specific transformant harboring the insertion was then identified, backcrossed (with strain 21gr) to generate a homogeneous genetic background, and then more fully characterized.

Figure 7A shows the positions of the *AphVIII* gene in the strains disrupted for *SLT1*, *SLT2*, and *SULTR2*. The Southern-blot analyses illustrated that *slt1*, *slt2*, and *sultr2* mutants all carry a single *AphVIII* insertion (Fig. 7B). These results were confirmed by genetic crosses of each single mutant with the wild-type strain, which demonstrated a 1:1 segregation ratio of paromomycin-resistant to paromomycin-sensitive progeny (data not shown). In the *slt1* mutant, the *AphVIII* construct was inserted in the eighth exon, interrupting the translation of a full-length product by introducing an incorrect splice site that caused a frame shift and the appearance of a premature stop codon (Supplemental Fig. S5A shows the alignment of the wild-type and



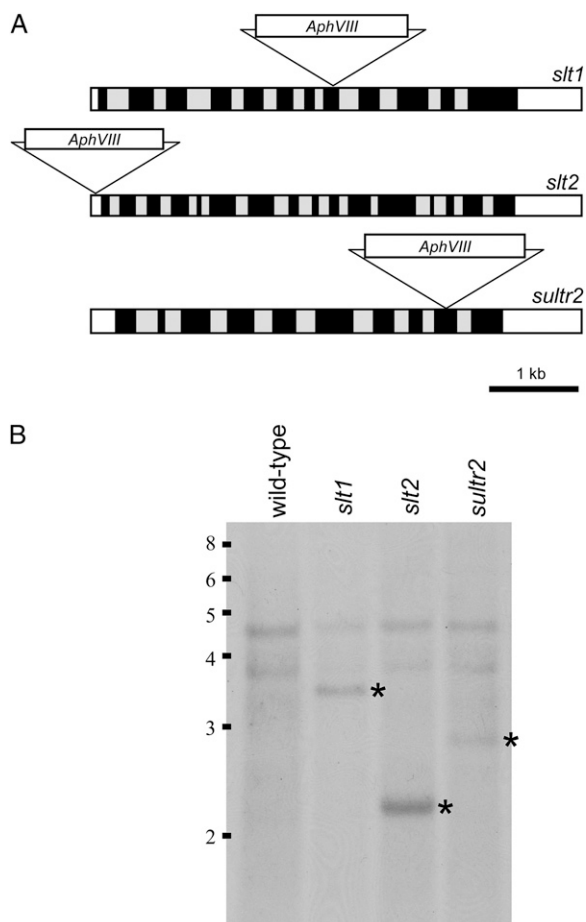


**Figure 7.** The copy number and position of the insertion of the *AphVIII* marker gene in the  $\text{SO}_4^{2-}$  transporter mutants. A, Diagram showing the site of *AphVIII* insertion in the *SLT1*, *SLT2*, and *SULTR2* genes. Black bars, gray bars, and white bars represent exons, introns, and untranslated regions, respectively. B, DNA gel-blot analysis of wild-type, *slt1*, *slt2*, and *sultr2* strains. Genomic DNA was digested with *Pst*I, separated by agarose gel electrophoresis, transferred to a nitrocellulose membrane, and hybridized with the 1.7-kb *PSAD::AphVIII* PCR fragment. Asterisks designate the newly introduced *PSAD::AphVIII* gene sequences. Size standards (in kb) are shown to the left.

truncated *SLT1* gene products). The aberrant *SLT1* transcript in the *slt1* mutant does not accumulate to the same extent as does the normal transcript in wild-type cells starved for S (the accumulation in the mutant is approximately 1 order of magnitude less than in the parental strain; Fig. 8A), suggesting that the mutation may also cause transcript instability. The lesion also abolished SLT1 protein accumulation during S deprivation, although a signal is observed when the general SLT antibody is used (Fig. 9A). Since the general SLT antibody recognizes both SLT1 and SLT2 polypeptides, the signal observed in the lane with polypeptides from the *slt1* mutant is likely to result from the presence of SLT2, as there is essentially no detectable SLT signal in a *slt1slt2* double mutant (Fig. 9B).

The integration site of the *AphVIII* gene in the *slt2* mutant is in the 5' untranslated region (Fig. 7), 38 bp

upstream of the translation start codon. Even though this disruption is not in the coding sequence, the accumulation of both the *SLT2* transcript and polypeptide are severely impacted by the mutation (Figs. 8A and 9A): essentially no SLT2 protein is detected in the mutant. We also observed a novel phenotype of the *slt2* mutant: the *SLT3* transcript, which decreased during S-limited growth of wild-type cells and the *slt1* and *sultr2* mutants, consistently increased in the *slt2* mutant (Fig. 8A).

In the *sultr2* mutant, a fragment of the *AphVIII* construct was inserted in the ninth exon of *SULTR2*, resulting in the generation of a chimeric transcript with a premature stop codon. The *SULTR2-AphVIII* transcript would be translated into a truncated polypeptide missing the last 115 amino acids of *SULTR2* (Supplemental Fig. S5B). This truncated polypeptide appears to be unstable and does not accumulate when the *sultr2* mutant is starved for S (Fig. 9A).

#### $\text{SO}_4^{2-}$ Uptake by the Mutant Strains

Prior to performing phenotypic analyses, each of the single mutants was backcrossed four times to the wild-type 21gr strain to eliminate other background mutations. The single mutants were then crossed to each other to generate double and triple mutants. The transcript and protein analyses for the strains with the multiple mutations are shown in Figures 8 and 9. There did not appear to be significant compensation for the absence of two S-deprivation-induced transporters in the double mutants; the level of transcript and polypeptide accumulation for the third transporter was similar to that observed in wild-type cells (Figs. 8B and 9B), based on normalization to the level of the *CBLP* transcript and *COX2b* protein, respectively. In order to assess whether the absence of specific  $\text{SO}_4^{2-}$  transporters impacted the rate of  $\text{SO}_4^{2-}$  transport, we measured the uptake rate of  $\text{SO}_4^{2-}$  over a range of external  $\text{SO}_4^{2-}$  concentrations (0.02–200  $\mu\text{M}$ ) in the wild type and the various mutant strains following S deprivation. As shown in Figure 10, the rates of  $\text{SO}_4^{2-}$  uptake in the *slt1*, *slt2*, and *sultr2* single mutants were not markedly depressed relative to that of wild-type cells. In contrast, the three double mutants all showed a significant decline (by approximately 50%) in their rate of  $\text{SO}_4^{2-}$  transport relative to wild-type cells. Most extreme was the phenotype of the triple *slt1slt2sultr2* mutant. This strain, which lacks all of the inducible transporters, exhibited a drastic decrease in the rate of  $\text{SO}_4^{2-}$  uptake. Indeed, the triple mutant exhibited essentially no increase in its  $\text{SO}_4^{2-}$  uptake capacity when deprived of S; the rate of  $\text{SO}_4^{2-}$  transport was the same in starved and unstarved cells (Fig. 10). Furthermore, wild-type cells and the *slt1slt2sultr2* triple mutant showed a similar rate of  $\text{SO}_4^{2-}$  transport under nutrient-replete conditions. The  $K_{1/2}$  was also calculated from the initial rates of  $\text{SO}_4^{2-}$  uptake for single, double, and triple mutants; we were unable to detect a significant difference in the transport affinity



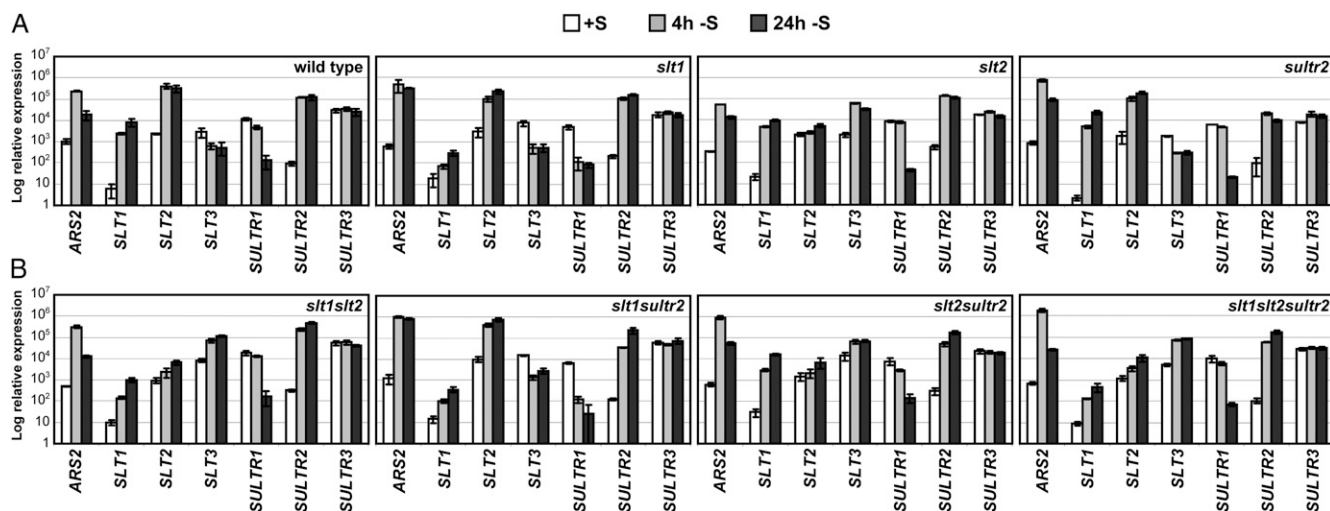


**Figure 8.** RT-qPCR for analysis of transcript accumulation in wild-type and mutant strains. The accumulation of *ARS2*, *SLT1*, *SLT2*, *SLT3*, *SULTR1*, *SULTR2*, and *SULTR3* transcripts is shown in wild-type cells and in the single (*slt1*, *slt2*, *sultr2*; A), double (*slt1slt2*, *slt1sultr2*, *slt2sultr2*), and triple (*slt1slt2sultr2*) mutants (B). RNA samples were collected prior to, and 4 and 24 h after, the cells were transferred from TAP to TAP-S medium. Levels of individual transcripts are given as relative abundance with respect to that of the housekeeping control gene (*CBLP*).

of wild-type cells relative to any of the mutant strains (Supplemental Table S3). This may not be too surprising for the single and double mutants, but the triple mutant also showed a decrease in the  $K_{1/2}$  that closely resembled that of wild-type cells. This might arise from the fact that the *slt2* mutation only affects transcript accumulation during S deprivation and does not disrupt the coding region; a small amount of SLT2 protein can still be translated from the basal level of *SLT2* transcript. In fact, a very weak signal using the SLT antibodies was detected in the *slt1slt2sultr2* mutant in S-depleted medium, which is likely from a low level of SLT2 polypeptide (Fig. 9B). Alternatively, posttranslational modifications of the transporters that function during S-replete growth may alter their kinetic characteristics, although they remain at low levels in the plasma membrane (so the  $V_{max}$  for uptake remains very low).

In order to confirm that the phenotype observed in the double and triple mutants is caused by the lesions in the  $\text{SO}_4^{2-}$  transporter genes, wild-type alleles of each transporter gene were introduced into the *slt1slt2sultr2* mutant background by a genetic cross to a wild-type strain (D66). The  $\text{SO}_4^{2-}$  uptake rates of the progeny correlated perfectly with the number of  $\text{SO}_4^{2-}$  transporter genes present in each strain (Supplemental Fig. S6, A and B). Note that the relative uptake rates of the single and double mutants are similar to the results presented in Figure 10, even though the absolute transport rates are lower in this experiment (due to the background difference between the 21gr and D66 strains). In sum, these results demonstrate that SLT1, SLT2, and SULTR2 are the prominent, high-affinity transporters involved in  $\text{SO}_4^{2-}$  uptake when the cells are deprived of S, while other transporters function during S-replete growth. Furthermore, there appears to

be some functional redundancy among the activities of these transporters.

## DISCUSSION

### $\text{SO}_4^{2-}$ Transporters in *Chlamydomonas*

One of the early responses of most organisms to S deprivation is the generation of high-affinity  $\text{SO}_4^{2-}$

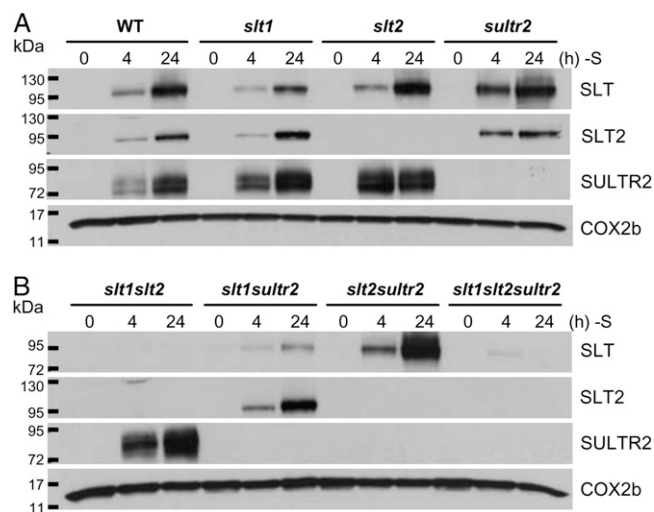


**Figure 9.** SULTR2, SLT1, and SLT2 polypeptide abundances in the  $\text{SO}_4^{2-}$  transporter mutants. A, The wild type (WT) and single mutants. B, The double and triple mutants. The time courses show the accumulation of SLT1, SLT2, and SULTR2 polypeptides following transfer of cells from S-replete to S-deficient medium. Samples were taken prior to, and 4 and 24 h after, the cells were transferred. The COX2b protein served as a loading control.

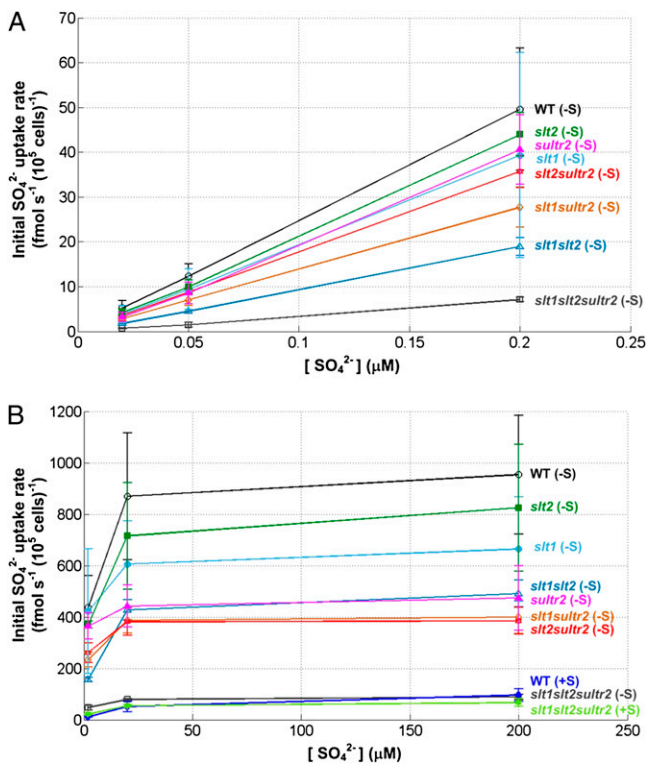


**Figure 10.** Characteristics of  $\text{SO}_4^{2-}$  transport in wild-type (WT) cells and single, double, and triple mutants in S-replete medium or medium devoid of S (deprived of S for 24 h). Transport assays were performed as a function of the external  $\text{SO}_4^{2-}$  concentrations: 0.02 to 0.2  $\mu\text{M}$  (A) and 2 to 200  $\mu\text{M}$  (B). Initial rates of uptake are expressed as  $\text{fmol SO}_4^{2-} \text{ s}^{-1} 10^5 \text{ cells}^{-1}$ . Values are averages of two to four biological replicates, and each biological experiment was performed in duplicate. Error bars represent 1 SD.

transport systems. In this study, we identified genes encoding plasma membrane  $\text{SO}_4^{2-}$  transporters and demonstrated that the activation of these genes occurred specifically during S deprivation. The elevated transcript accumulation was detected 1 to 2 h after transferring cells to medium devoid of S (Fig. 2). It is noteworthy that the transcripts encoding the high-affinity  $\text{SO}_4^{2-}$  transporters accumulate significantly more rapidly than transcripts encoding other S-responsive genes, such as *ARS2* and *ECP76*, following the transfer of cells to -S medium (Takahashi et al., 2001). These results suggest that there is a tiered regulation of the S-responsive genes and that the induction of the high-affinity  $\text{SO}_4^{2-}$  transport system is one of the earliest responses to S starvation. A distinct permease involved in translocating  $\text{SO}_4^{2-}$  from the cytoplasm into chloroplasts is composed of the subunits SulP1, SulP2, Sabc, and Sbp (Melis and Chen, 2005). Expression of all four genes encoding the components of this permease is induced upon S deprivation; levels of SulP and Sabc polypeptides also increase when the cells become S limited (Lindberg and Melis, 2008).

In addition, S-starved cells exhibit increased  $\text{SO}_4^{2-}$  uptake activity within 1 h of the onset of S deprivation (Yildiz et al., 1994). This initial increase in uptake rate precedes the accumulation of newly synthesized  $\text{SO}_4^{2-}$  transporters (Fig. 4B), suggesting that there might also be posttranslational modifications of the existing  $\text{SO}_4^{2-}$  transporters. This suggestion is in accord with the finding that the  $K_{1/2}$  for  $\text{SO}_4^{2-}$  transport in the *slt1slt2sultr2* triple mutant still rapidly changes following the imposition of S deprivation; the  $V_{\text{max}}$  remains low because the three S-responsive transporters are not synthesized. Finally, transcripts for two putative  $\text{SO}_4^{2-}$  transporters, *SULTR1* and *SLT3*, decline during S deprivation. The encoded proteins may have low-affinity transporter activity that is likely to primarily function in the uptake of  $\text{SO}_4^{2-}$  under S-replete conditions.

Intriguingly, *Chlamydomonas* has both  $\text{H}^+/\text{SO}_4^{2-}$  cotransporters (SULTR) and  $\text{Na}^+/\text{SO}_4^{2-}$  transporters (SLT), while vascular plants such as *Arabidopsis* has only retained the  $\text{H}^+/\text{SO}_4^{2-}$  cotransporters. This finding suggests that *Chlamydomonas* diverged from the plant lineage (approximately 1 billion years ago) prior to the loss of the  $\text{Na}^+/\text{SO}_4^{2-}$  transporters. Furthermore, some  $\text{SO}_4^{2-}$  transporters in *Chlamydomonas* appear to have arisen from a recent duplication, since closely related organisms such as *Volvox carteri* and the marine chlorophyte *Ostreococcus tauri* appear to have fewer transporters. For example, *Volvox* appears to have one  $\text{H}^+/\text{SO}_4^{2-}$  and two  $\text{Na}^+/\text{SO}_4^{2-}$  cotransporters, and *Ostreococcus* has only two  $\text{Na}^+/\text{SO}_4^{2-}$  transporters; *Chlamydomonas* has three members for each of those protein families. Retention of the  $\text{Na}^+/\text{SO}_4^{2-}$  transporters in *Ostreococcus* may reflect the fact that it would not be energetically favorable to use  $\text{H}^+$ -coupled  $\text{SO}_4^{2-}$  transport in the oceans where  $\text{Na}^+$  concentrations are high. In addition, *Volvox* may not require a large set of  $\text{SO}_4^{2-}$  transporter proteins, since it has an extensive extracellular matrix that could potentially store significant amounts of S. The inability of *Chlamydomonas* to store S and perhaps other nutrients may have favored the selection of strains in which there was an expansion of families of genes encoding nutrient transport proteins. Furthermore, retaining both the  $\text{Na}^+/\text{SO}_4^{2-}$  and  $\text{H}^+/\text{SO}_4^{2-}$  transporter types may allow *Chlamydomonas* to survive under diverse environmental conditions. The  $\text{H}^+/\text{SO}_4^{2-}$  transporters may be primarily used when the pH of the milieu around the cell is low, while the  $\text{Na}^+/\text{SO}_4^{2-}$  cotransporters may be responsible for the majority of  $\text{SO}_4^{2-}$  uptake when the pH is high and when it is more efficient to use  $\text{Na}^+$  as a counter ion.

The *SLT2* and *SLT3* genes are tandemly arranged on chromosome 10 in a head-to-tail orientation; the 3' untranslated region of *SLT2* overlaps with the 5' untranslated region and the first exon of *SLT3*. In wild-type cells, *SLT2* is heavily transcribed during S deprivation, and this likely interferes with the transcription of the downstream *SLT3* gene, resulting in a decrease in *SLT3* mRNA abundance (Fig. 8). In

contrast, transcriptional activity of *SLT2* in the *slt2* mutant is decreased due to the insertion in the 5' untranslated region, which probably accounts for an unusually high rate of *SLT3* transcription during S deprivation. Interestingly, *SLT2* and *SLT3* (76% identity, 85% similarity to each other) have a similar exon-intron organization, suggesting that they arose from a gene duplication, but based on their unique expression patterns, the genes have subsequently specialized (Fig. 3A). Finally, the SLT and SULTR protein families each likely contains both high- and low-affinity transporters, allowing Chlamydomonas to tailor uptake processes to the features of the environment under both high- and low-S conditions.

### Transcriptional Regulation of $\text{SO}_4^{2-}$ Transporters

Several isoforms of  $\text{SO}_4^{2-}$  transporters play important roles in facilitating  $\text{SO}_4^{2-}$  uptake during S deprivation in Arabidopsis. The S-responsive induction of these transporter genes (*AtSULTR1;1*, *AtSULTR1;2*, *AtSULTR4;2*) has been shown to be under the control of SLIM1, the ETHYLENE-INSENSITIVE-LIKE3 transcriptional regulator (Maruyama-Nakashita et al., 2006). As already mentioned, a number of factors associated with S-responsive regulation in Chlamydomonas have also been identified; these include SNRK2.1, SNRK2.2, and SAC1. Mutants devoid of these regulatory elements show aberrant responses to S deprivation (Gonzalez-Ballester and Grossman, 2009). We examined the accumulation of  $\text{SO}_4^{2-}$  transporter transcripts in wild-type cells and the *sac1* and *snrk2.1* mutants; these mutant strains do not elevate  $\text{SO}_4^{2-}$  transport activity nearly as much as wild-type cells when they are deprived of S (Fig. 1). In contrast to wild-type cells, the *sac1* mutant only accumulates *SLT1*, *SLT2*, and *SULTR2* transcripts 24 h after the imposition of S starvation. This is consistent with the model proposed by Moseley et al. (2009), in which SAC1 is a sensor that resides on the plasma membrane and acts as a negative regulator of the SNRK2.2 repressor protein kinase when environmental  $\text{SO}_4^{2-}$  levels fall below a certain threshold. This causes derepression of the S-responsive genes, including those encoding  $\text{SO}_4^{2-}$  transporters. After a prolonged period of S starvation, intracellular  $\text{SO}_4^{2-}$  levels also decline and further stimulate the transcription of S-responsive genes as a consequence of activation of the SNRK2.1 activator protein kinase; such activation can occur in the *sac1* mutant, leading to elevated accumulation of  $\text{SO}_4^{2-}$  transporter mRNA 24 h after the onset of S starvation (Fig. 3B), which then leads to increases in the levels of transporter protein (Supplemental Fig. S2) and uptake activity (Fig. 1), although both are still lower than in wild-type cells.

Similarly, the *snrk2.1* mutant is severely compromised in its ability to increase the rate of  $\text{SO}_4^{2-}$  uptake during S starvation (Fig. 1); its phenotype is significantly more severe than that of the *sac1* mutant. The abundance of *SLT1*, *SLT2*, and *SULTR2* transcripts

in the *snrk2.1* mutant, under both S-replete and S-depleted conditions, is much lower than the levels observed in wild-type cells (Fig. 3). For *SULTR2*, expression is induced in the *snrk2.1* mutant during S deprivation, but the basal and fully induced transcript levels are both much lower than observed in wild-type cells. The *SLT1* transcript does not accumulate in this mutant. These results suggest that SNRK2.1 is critical for maintaining both basal-level expression and the accumulation of *SLT1* and *SULTR2* transcripts during acclimation of the cells to S deprivation. Similar to the situation in the *sac1* mutant, the inability of *snrk2.1* to induce  $\text{SO}_4^{2-}$  transport activity during S deprivation is associated with its failure to accumulate  $\text{SO}_4^{2-}$  transporter transcripts. The capacity for  $\text{SO}_4^{2-}$  transport in wild-type, *sac1*, and *snrk2.1* cells starved for S generally correlates with the levels of transcript and transporter polypeptide accumulation (Figs. 1 and 4; Supplemental Fig. S2). Together, these results indicate that *SLT1*, *SLT2*, and *SULTR2* encode high-affinity  $\text{SO}_4^{2-}$  transporters that are controlled by the S status of the environment at the level of transcript abundance and that are responsible for the majority of  $\text{SO}_4^{2-}$  uptake when the cells become S deprived.

In contrast, the *SULTR1* and *SLT3* genes appear to be down-regulated during S starvation (the transcripts are reduced by 1,000- and 10-fold, respectively; Fig. 3A), suggesting that the proteins encoded by these genes are low-affinity  $\text{SO}_4^{2-}$  transporters that function primarily under S-sufficient conditions. Furthermore, S deprivation does not cause a significant reduction in *SULTR1* and *SLT3* transcript abundance in the *sac1* mutant, while these transcripts are elevated to some extent in the *snrk2.1* strain (Fig. 3, B and C). Hence, SAC1 and SNRK2.1 are important not only for stimulating the activity of the *SLT1*, *SLT2*, and *SULTR2* genes but are also involved in depressing the activities of the *SULTR1* and *SLT3* genes during S limitation.

Even though the *SULTR3* transcript does not appear to be regulated by the S status of the cells, its level accumulates during S starvation in a *snrk2.1* background (Fig. 3, A and C). The inability of the *snrk2.1* mutant to up-regulate expression of the high-affinity transporters and other genes involved in the acclimation program may result in severe internal S starvation that elicits secondary effects, including an increase in *SULTR3* transcript accumulation. Alternatively, SNRK2.1 may play a direct role in regulating *SULTR3* expression.

### Accumulation and Turnover of $\text{SO}_4^{2-}$ Transporters

*SLT1*, *SLT2*, and *SULTR2* polypeptides accumulate in S-starved cells 1 to 2 h after the transcripts peak (Fig. 4). These proteins are synthesized de novo upon imposition of S deprivation, since administration of CHX at the time of transferring cells from S-replete to S-depleted medium blocked their accumulation (Supplemental Fig. S3). Moreover, these  $\text{SO}_4^{2-}$  transporters are turned over rapidly when S becomes available;

they are almost undetectable 8 h after  $\text{SO}_4^{2-}$  is added to S-starved cultures (Fig. 4B). The half-lives of SLT1, SLT2, and SULTR2 are two to three times longer in the absence of  $\text{SO}_4^{2-}$ ; the rate of turnover increases when the cells are placed in S-rich medium (Fig. 5). These data strongly suggest that de novo synthesis of SLT1, SLT2, and SULTR2 specifically facilitates  $\text{SO}_4^{2-}$  transport when cells experience S starvation. Once starvation conditions are relieved, these high-affinity transporters are rapidly degraded, with S (either  $\text{SO}_4^{2-}$  or a reduced S metabolite) stimulating the degradation process. The proteasome is involved in degrading SLT1 and SLT2, although it is not known whether the involvement is direct or indirect. Surprisingly, proteasome activity does not appear to be required for SULTR2 degradation. There are several examples of the degradation of plasma membrane transporter polypeptides by mono-ubiquitination and subsequent proteasome-independent proteolysis in vacuoles (Eguez et al., 2004; Wolf, 2004). Tight regulation of high-affinity transporter synthesis and turnover that depends on S availability would allow for an economy of energy utilization by the cells, balancing the transport process with intracellular demand, and might also help control the uptake of selenate, a toxic analog of  $\text{SO}_4^{2-}$ , under all environmental conditions. In addition, the high-affinity  $\text{SO}_4^{2-}$  transporters may have a lower capacity for  $\text{SO}_4^{2-}$  uptake than the low-affinity transporters (SULTR1 and SLT3), making them less suitable for  $\text{SO}_4^{2-}$  uptake when there is an abundance of the anion in the environment.

#### Localization of SLT1, SLT2, and SULTR2 on the Plasma Membrane and Their Role in $\text{SO}_4^{2-}$ Uptake

To facilitate  $\text{SO}_4^{2-}$  uptake from the environment, algal and plant cells must have the capacity to synthesize high-affinity  $\text{SO}_4^{2-}$  transporters, some of which must reside on the plasma membrane. Using two-phase aqueous polymer separation coupled with Suc density gradient centrifugation, we demonstrated that all three of the S-deprivation-induced transporters, SLT1, SLT2, and SULTR2, reside in the plasma membrane (Fig. 6). Expression of the cDNAs encoding these transporters in the yeast  $\text{SO}_4^{2-}$  transporter mutant CP60-1C failed to rescue its growth phenotype (Supplemental Table S1). While it was possible that the difference in Chlamydomonas and yeast codon usage could result in heterologous expression problems, this is probably not the case, since, as shown in Supplemental Figure S4A, the Chlamydomonas  $\text{SO}_4^{2-}$  transporter-GFP fusion proteins accumulated in the yeast transformants. However, the GFP fluorescence in yeast cells expressing the Chlamydomonas SULTR2-, SLT1-, and SLT2-GFP fusion proteins accumulates within intracellular membranes that probably originate from the endoplasmic reticulum (Supplemental Fig. S4B, I, II, and III). In contrast, in CP60-1C cells harboring AtSULTR1;2 fused to GFP, much of the fluorescence signal is distributed over the cell surface (Supplemen-

tal Fig. S4B, IV). These results suggest that our inability to complement the yeast mutant is a consequence of inefficient localization of the Chlamydomonas transporters to the yeast plasma membrane. Perhaps plasma membrane localization of Chlamydomonas  $\text{SO}_4^{2-}$  transporters requires a posttranslational modification (e.g. phosphorylation) that does not occur in yeast cells. Recently, phosphorylation of the yeast nitrate transporter Ynt1 has been shown to be essential for its delivery to the plasma membrane during N limitation (Navarro et al., 2008). Similarly, phosphorylation of the yeast plasma membrane ATPase is critical for its proper maturation and routing to the cell surface (DeWitt et al., 1998). Alternatively, Chlamydomonas transporters may require an accessory protein in the secretory pathway for proper targeting. The PHOSPHATE TRANSPORTER TRAFFIC FACILITATOR1, a plant-specific SEC12-related protein, has been demonstrated to play a critical role in facilitating endoplasmic reticulum exit of a high-affinity phosphate transporter in Arabidopsis (Gonzalez et al., 2005).

We also attempted to express Chlamydomonas  $\text{SO}_4^{2-}$  transporters in *Xenopus* oocytes but never succeeded in obtaining oocytes with an increased rate of  $\text{SO}_4^{2-}$  uptake (data not shown). These results, along with those of the experiments described for heterologous expression of the Chlamydomonas transporters in the yeast system, suggested that there are biogenesis-specific processes that are required for proper maturation/localization of Chlamydomonas transporters. Intriguingly, while none of the high-affinity  $\text{SO}_4^{2-}$  transporters from Chlamydomonas was able to complement the CP60-1C strain,  $\text{SO}_4^{2-}$  transporters of Arabidopsis (SULTR1;1, SULTR1;2, and SULTR1;3) do rescue the yeast mutant phenotype (Supplemental Table S1; Takahashi et al., 2000; Shibagaki et al., 2002; Kataoka et al., 2004a). These results suggest that Chlamydomonas and Arabidopsis, which diverged over 1 billion years ago (Merchant et al., 2007), have different posttranslational modifications, stabilities, and/or mechanisms by which the transporters are localized to the plasma membrane.

Since we were unable to confirm the functionality of SULTR2, SLT1, and SLT2 in the heterologous systems, Chlamydomonas mutants with insertions in the  $\text{SO}_4^{2-}$  transporter genes were identified by a PCR-based screen (Fig. 7) and characterized at the physiological level by measuring  $\text{SO}_4^{2-}$  uptake rates in the various strains (Fig. 10). The results clearly show that the transporters are critical for the uptake and assimilation of  $\text{SO}_4^{2-}$  in S-deprived cells and that there is some functional redundancy among the transporters. Interestingly, in the S-starved *sultr2* mutant, the uptake rates at low external  $\text{SO}_4^{2-}$  concentrations (0.02–2  $\mu\text{M}$ ) are comparable to those of wild-type cells, while the transport rates at higher  $\text{SO}_4^{2-}$  concentrations (20–200  $\mu\text{M}$ ) are much lower than the rates in the wild-type strain, suggesting that SULTR2 may be responsible for much of the  $\text{SO}_4^{2-}$  uptake into S-deprived cells.

Remarkably, increased uptake capacity normally observed during S deprivation is completely abolished in the triple mutant (Fig. 10B); the maximal  $\text{SO}_4^{2-}$  uptake rates of the *slt1slt2sultr2* mutant during S-replete and S-depleted conditions are essentially the same. These data suggest that SLT1, SLT2, and SULTR2 are responsible for essentially all induced  $\text{SO}_4^{2-}$  uptake that is associated with S deprivation.

## MATERIALS AND METHODS

### Strains and Growth Conditions

The following *Chlamydomonas reinhardtii* strains were used: 21gr (available from the Chlamydomonas Center), D66 (*nit2<sup>-</sup>*, *cw15*, *mt<sup>+</sup>*; Pollock et al., 2003), *sac1* (Davies et al., 1996), and *snrk2.1* (*ars11* allele; Gonzalez-Ballester et al., 2008). Cells were cultured in either S-replete or S-depleted (–S) Tris-acetate-phosphate (TAP) medium under continuous illumination ( $80 \mu\text{mol photons m}^{-2} \text{s}^{-1}$ ) on a rotating platform (200 rpm) at 25°C. TAP–S medium was prepared as described previously (Davies et al., 1994). For S-starvation experiments, cells were grown to midlogarithmic phase ( $2\text{--}4 \times 10^6$  cells  $\text{mL}^{-1}$ ) in TAP medium, washed once with TAP–S medium (2,500g for 5 min), and resuspended in TAP–S to the original cell density. For transformation experiments, *Chlamydomonas* cells were grown in TAP medium to a density of  $2$  to  $4 \times 10^6$  cells  $\text{mL}^{-1}$ . Transformants were selected on TAP plates supplemented with  $5 \mu\text{g mL}^{-1}$  paromomycin, as described previously (Davies et al., 1996; Pollock et al., 2005).

### Isolation of *SLT1*, *SLT2*, and *SULTR2* cDNAs

Total RNA was isolated from 12-h S-starved 21gr (wild-type) cells using a standard phenol-chloroform extraction protocol (Sambrook et al., 1989). Reverse transcription and PCR were performed using the Sensiscript RT Kit (Qiagen) and *Pfu* Turbo DNA Polymerase (Stratagene). Amplified PCR products were cloned into pENTR-D-TOPO (Invitrogen) and sequenced.

### $\text{SO}_4^{2-}$ Uptake Assays

$\text{SO}_4^{2-}$  transport assays were performed as described previously (Yildiz et al., 1994). The rate of  $\text{SO}_4^{2-}$  uptake was measured at the indicated external concentrations of the anion over a 2-min time series.

### RNA Isolation and Quantification

Total RNA was extracted from frozen cell pellets using the RNeasy Mini Kit (Qiagen) and treated with RNase-free DNase I (Qiagen) to remove residual genomic DNA. First-strand cDNA was synthesized from 3 to 5  $\mu\text{g}$  of total RNA using oligo(dT)<sub>12–18</sub> for priming the SuperScript III reverse transcriptase reaction, as described in the manual (Invitrogen). RT-qPCR was performed with a Roche LightCycler 480. PCRs were in a final volume of 20  $\mu\text{L}$  composed of 10  $\mu\text{L}$  of LightCycler 480 SYBR Green Master Mix (Roche), 5  $\mu\text{L}$  of a 1:50 cDNA dilution, 400 nm of each primer, and distilled water to make up the remainder of the 20- $\mu\text{L}$  volume. Conditions used for amplification in the thermocycler were as follows: preincubation at 95°C for 5 min, followed by 50 cycles of denaturation at 95°C for 10 s, annealing at 60°C for 20 s, elongation at 72°C for 20 s, and measurement of fluorescence after 80°C for 5 s (the last step was incorporated into the protocol to avoid background signals resulting from the formation of primer dimers). A melt-curve analysis program (60°C–99°C, heating rate of  $2.2^\circ\text{C s}^{-1}$ , and continuous fluorescence measurements) was used to evaluate the specificity of the amplification reactions. All reactions were performed in triplicate with at least two biological replicates. The *CBLP* gene was used as a housekeeping gene control (Chang et al., 2005). The primer pairs used for RT-qPCR analysis were 5'-CTTCTCGCCCATGACCAC-3' and 5'-CCCACCAGGTGGTCTTCAG-3' for *CBLP*; 5'-CTTAATTGCATGCGCGCCGTCA-3' and 5'-TCAGAACACCAACGCAAGTTCCAG-3' for *ARS2*; 5'-TGGCCATGCTTATCGTCATCTATG-3' and 5'-TCGATGCGCATGACCA-GGAT-3' for *SULTR1*; 5'-ACGTGGCATGCGACTCAT-3' and 5'-CTTGCCACTTTGCCAGGT-3' for *SULTR2*; 5'-AAGCTGGACCGGTGGTGAGAA-3'

and 5'-TCACATGTCAGTGCACGCCAG-3' for *SULTR3*; 5'-ACGGGTTCTT-CGAGCGAATTGC-3' and 5'-CGACTGCTTACGCAACAATCTTGG-3' for *SLT1*; 5'-GTACGGAGTTCCTTACGCG-3' and 5'-TTCTTCGCCACCGATG-AGC-3' for *SLT2*; 5'-CCCAGTCTTTGGCGCAAG-3' and 5'-GGCCTACT-CGCTACCCTACC-3' for *SLT3*; 5'-GCGCTGCCCTCCGTACCTCC-3' and 5'-CAGCCGCACGCCGTCCAGTAG-3' for *NIT1*; and 5'-TTCCGTTTCCG-TTCTCTGAC-3' and 5'-CCCTGCATCTGTCTCCAG-3' for *PHOX*.

### Peptide Synthesis and Antibody Production

Specific antibodies against FOX1, CRD1, and COX2b were kind gifts from Dr. Sabeeha Merchant (University of California, Los Angeles). The antibodies to SULTR2 and SLT2 were prepared by Agrisera, while the SLT general antibody was prepared by Covance Research Products. Monospecific antibodies for SLT2 were generated in rabbits against a peptide region (DGKYLKSPDPNW) unique to this transport protein (Supplemental Fig. S1B). This peptide was conjugated to keyhole limpet hemocyanin via a terminal Cys and injected into rabbits. Resulting antibodies were affinity purified by column chromatography using an UltraLink Iodoacetyl Gel (Pierce) covalently bound to the unique SLT2 peptide used for antibody production. SLT2 peptide synthesis, peptide conjugation, antibody production, and antibody purification were all performed by Agrisera. To generate polyclonal antibodies that specifically recognize SULTR2, a cDNA encoding a unique region in the SULTR2 protein (Glu-677 to Gln-764; Supplemental Fig. S1A) was cloned in frame into the 3' terminus of the 10×His-encoding sequence of the expression vector pET-16b (Novagen) and introduced into *Escherichia coli* for isopropylthio- $\beta$ -galactoside-inducible expression. *E. coli* cells expressing the fusion protein were grown to an  $A_{600}$  of 0.5 and then induced with isopropylthio- $\beta$ -galactoside for 4 h at 37°C. The 10×His-SULTR2 protein was purified using a nickel-nitrilotriacetic acid agarose Superflow column (Qiagen) and then subjected to preparative SDS-PAGE (15% polyacrylamide gel). The region of the gel containing the fusion protein was excised and used for antiserum production in rabbits. To generate general antibodies that would react with both SLT1 and SLT2 (and potentially with SLT3), cDNAs encoding the region of SLT1 and SLT2 from Thr-337 to Val-584 (Supplemental Fig. S1B) were cloned into pET-16b (the SLT1 and SLT2 amino acid sequences from this region are 91% identical and 97% similar). These expressed 10×His-SLT1- and 10×His-SLT2-tagged polypeptides were resolved by preparative SDS-PAGE, as described above, and regions of the gel containing the fusion proteins were excised and used as antigens for antibody production.

### Protein Isolation, SDS-PAGE, and Immunoblot Analysis

*Chlamydomonas* cells ( $2\text{--}4 \times 10^6$  cells  $\text{mL}^{-1}$  in 100 mL) were collected by centrifugation (3,000g, 5 min) and resuspended in 0.1 M sodium phosphate buffer (pH 7.0). Chlorophyll was extracted from the cells into 80% acetone and 20% methanol, and its concentration was determined spectrophotometrically (Arnon, 1949) after removal of cell debris and denatured proteins by centrifugation. Quantities of cells with equal chlorophyll content (200–300  $\mu\text{g}$ ) were pelleted, resuspended in an ice-cold homogenization buffer (0.25 M Suc, 0.1 M HEPES, pH 7.5, 15 mM EGTA, 5% glycerol, and 0.5% polyvinylpyrrolidone) containing a protease inhibitor cocktail (Sigma), and then disrupted by agitation with glass beads (425–600  $\mu\text{m}$ ). After removal of cell debris by a brief centrifugation (2,000g, 5 min), the supernatant was centrifuged at 100,000g for 50 min to obtain a microsomal pellet, which was then resuspended in the homogenization buffer containing 1% Triton X-100. An equal volume of loading buffer (6.25 mM Tris-HCl, pH 6.8, 5% SDS, 6 M urea, 500 mM dithiothreitol, 10% glycerol, and 0.002% bromophenol blue) was added to the samples prior to an incubation at 42°C for 15 min. Solubilized polypeptides were resolved by SDS-PAGE on a 10% polyacrylamide gel and transferred to polyvinylidene difluoride membranes using a wet transfer method. Blots were blocked in 5% milk in Tris-buffered saline solution with 0.1% Tween 20 prior to 1 h of incubation in the presence of primary antibodies. The dilutions of the primary antibodies used were as follows: 1:2,500 anti-SULTR2, 1:3,000 anti-SLT, 1:1,000 anti-SLT2, 1:1,000 anti-FOX1, 1:1,000 anti-H<sup>+</sup>-ATPase (Agrisera), 1:1,000 anti-V-ATPase (Agrisera), 1:3,000 CRD1, and 1:40,000 anti-COX2b. A 1:10,000 dilution of horseradish peroxidase-conjugated anti-rabbit IgG (Promega) was used as a secondary antibody. The peroxidase activity was detected by an enhanced chemiluminescence assay (Amersham Biosciences).

### Cell Treatment

CHX, which inhibits protein synthesis on 80S ribosomes, was used at a final concentration of 10  $\mu\text{g mL}^{-1}$ . This concentration effectively inhibits

protein synthesis in *Chlamydomonas* (Kawazoe et al., 2000). The proteasome inhibitor MG132 (carbobenzoxy-leucyl-leucyl-leucinal; Sigma) was added to a final concentration of 10  $\mu\text{M}$  (Smalle and Vierstra, 2004).

## Plasma Membrane Isolation

The D66 strain was used for plasma membrane isolations. Ten liters of cells were grown to midlogarithmic phase ( $3 \times 10^6$  cells  $\text{mL}^{-1}$ ) in a stirred bottle and starved for 5 to 24 h. Batches of resuspended cells (from 10 g pellet wet weight) were sonicated on ice using a Fisher Scientific Sonic Dismembrator model 550 with a microtip probe, power setting 3.5, and 15 cycles of 1 min of sonication, each followed by 1 min of cooling. The total microsomal fraction was separated into plasma membranes and a fraction containing the rest of the membranes using a two-phase aqueous polymer system described by Herbig et al. (2002). To fractionate membrane protein from the top (polyethylene glycol) phase of the two-phase aqueous polymer system, 600  $\mu\text{g}$  of protein was loaded onto a 4.5-mL, 15% to 45% Suc gradient and centrifuged at 4°C for 16 h at 31,000 rpm in SW60Ti rotor (Beckman Coulter). The gradient was separated into 11 fractions of equal volume, diluted 5-fold in a dilution buffer (5 mM MOPS, pH 7.0, 2 mM dithiothreitol, 1 mM EDTA, and 1 mM phenylmethylsulfonyl fluoride), and centrifuged at 4°C for 1 h at 50,000 rpm in the TLA100.3 rotor (Beckman Coulter). Pellets were resuspended in 50  $\mu\text{L}$  of the dilution buffer, and an equal volume of the loading buffer was added to the samples prior to an incubation at 42°C for 15 min. SDS-PAGE and immunoblot analyses were performed as described above.

## Generation of *Chlamydomonas* Mutants

To generate a library of insertional mutants, a 1.7-kb PCR fragment containing the selectable marker gene *AphVIII* (conferring resistance to paromomycin; Sizova et al., 2001) under the control of the *PSAD* promoter was used for transformation. The cell wall-less strain D66 was transformed by electroporation (Shimogawara et al., 1998) using a modified procedure reported by Colombo et al. (2002). After transformation, cells were incubated in TAP medium for 16 to 18 h to allow for the accumulation of the *AphVIII* protein. Transformants were subsequently selected on TAP medium supplemented with 5  $\mu\text{g mL}^{-1}$  paromomycin.

## Generation and Screening of the Mutant Library

The mutant screen was performed according to Gonzalez-Ballester (2005). In brief, transformants were generated as described above, transferred to 96-well microtiter plates containing approximately 100  $\mu\text{L}$  of liquid TAP medium, grown for 5 d before they were used for genomic DNA isolation; the plates were wrapped in Parafilm to minimize evaporation. Each microtiter plate represents a pool of 96 insertional mutants. Genomic DNA was isolated from a pool of 96 transformants using a standard phenol-chloroform protocol (Sambrook et al., 1989). An equal concentration of genomic DNA from 10 pools was combined to create a "superpool" of DNA at a concentration of 100 ng  $\mu\text{L}^{-1}$ . To screen for mutants of interest, the superpool DNA was used as a template for PCR. Each PCR was performed using one gene-specific primer (the gene for which a disruption is sought; Supplemental Table S2) and one *AphVIII* construct-specific primer (RB2, 5'-TACCGGCTGTGGAC-GAGTCTCTCTG-3'). Multiple gene-specific primers were paired with the *AphVIII* primer to increase our chances of identifying a disrupted target gene. PCRs were performed in a final volume of 25  $\mu\text{L}$  containing 0.2  $\mu\text{L}$  of *Taq* DNA Polymerase (Qiagen), 2.5  $\mu\text{L}$  of  $10\times$  PCR buffer, 2  $\mu\text{L}$  of deoxyribonucleotide triphosphates (2.5 mM each), 4  $\mu\text{L}$  of Q solution (Qiagen), 1  $\mu\text{L}$  of dimethyl sulfoxide (Sigma), 1  $\mu\text{L}$  of template, 400 nM of each primer, and distilled water to make up the remainder of the 25- $\mu\text{L}$  volume. Conditions used for amplification in the thermocycler were as follows: preincubation at 95°C for 5 min, followed by 35 cycles of sequential denaturation at 95°C for 30 s, annealing at 60°C for 30 s, and amplification at 72°C for 120 s. PCR products were separated by gel electrophoresis using 0.8% agarose gels. To identify DNA regions adjacent to the right border of the *AphVIII* construct (downstream from the *PSAD* promoter), the PCR product amplified with the gene-specific primer and RB2 was excised from the gel, purified using the QIAquick PCR Purification Kit (Qiagen), and sequenced. Primers used for this screening are listed in Supplemental Table S2.

## Southern-Blot Analyses

Genomic DNA was isolated from 50-mL liquid cultures of the wild-type strain 21gr and *slt1*, *slt2*, and *sultr2* mutants using a standard phenol-

chloroform extraction protocol (Sambrook et al., 1989). Ten micrograms of genomic DNA was digested for 20 h with 10 units of restriction endonucleases (*PstI*; New England Biolabs). The fragments were separated by agarose (0.8%) gel electrophoresis and blotted overnight in  $20\times$  SSC onto nylon membranes (GeneScreen; DuPont-New England Nuclear), and the transferred DNA was cross-linked to the membrane by UV illumination. An alkaline phosphatase-labeled probe was synthesized by chemical cross-linking of a thermostable alkaline phosphatase to the nucleic acid template. Probe synthesis and hybridization were performed using the AlkPhos Direct Labeling and Detection Systems following the manufacturer's protocol (Amersham Biosciences).

## Rescue of the Mutant Phenotype

The phenotype of the *slt1slt2sultr2* mutant was rescued by introducing wild-type alleles encoding the individual transporters into the triple mutant background. The *slt1slt2sultr2* strain was crossed to the D66 wild-type strain, and the  $\text{SO}_4^{2-}$  transport rate of the progeny containing one (*slt1*, *slt2*, or *sultr2*) or two (*slt1slt2*, *slt1sultr2*, or *slt2sultr2*) mutations was determined by  $\text{SO}_4^{2-}$  uptake assays.

Sequence data from this article can be found in the GenBank/EMBL data libraries under accession numbers NM\_179568 (*AtSULTR1;2*), CAA57710 (*ShSHST1*), XP\_001766939 (putative  $\text{SO}_4^{2-}$  permease from *Physcomitrella patens*), GU181275 (*SLT1*), GU181276 (*SLT2*), and GU181277 (*SULTR2*).

## Supplemental Data

The following materials are available in the online version of this article.

**Supplemental Figure S1.** Amino acid sequence alignment of  $\text{SO}_4^{2-}$  transporter proteins.

**Supplemental Figure S2.** *SULTR2*, *SLT1*, and *SLT2* polypeptide abundances in wild-type 21gr (WT), *sac1*, and *snrk2.1* strains.

**Supplemental Figure S3.** CHX inhibition of accumulation of the  $\text{SO}_4^{2-}$  transporter protein during S deprivation.

**Supplemental Figure S4.** Expression of  $\text{SO}_4^{2-}$  transporter-GFP fusion proteins in *S. cerevisiae* cells.

**Supplemental Figure S5.** Amino acid sequence alignments of *SLT1* and *SULTR2* wild-type and mutant gene products.

**Supplemental Figure S6.** Characteristics of  $\text{SO}_4^{2-}$  transport in wild-type cells and single, double, and triple  $\text{SO}_4^{2-}$  transporter mutants (progeny of a cross between a wild-type strain and a *slt1slt2sultr2* triple mutant) deprived of S for 24 h.

**Supplemental Table S1.** Growth rates of the CP60-1C strain harboring genes encoding Arabidopsis *SULTR1;2* or various *Chlamydomonas*  $\text{SO}_4^{2-}$  transporters.

**Supplemental Table S2.** List of *SULTR2*-, *SLT1*-, and *SLT2*-specific primers used for PCR screening of the insertion library.

**Supplemental Table S3.** Characteristics of  $\text{SO}_4^{2-}$  transport in wild-type cells and the single, double, and triple  $\text{SO}_4^{2-}$  transporter mutants after 24 h of S deprivation.

**Supplemental Materials and Methods S1.**

## ACKNOWLEDGMENTS

We thank Dr. Nakako Shibagaki, Dr. Jeffrey Moseley, and Dr. Florence Mus for valuable discussions of the results and all members of the Grossman and Bhaya laboratories for support and advice. We thank Ariana Afshar, Matthew Prior, and Leonardo Magneschi for their help with the mutant screen. We also thank Dr. Sheng Luan and Dr. Wenzhi Lan for their help with the *Xenopus* oocyte experiment and Dr. Mark Dudley Page for his advice on the plasma membrane isolation. The antibodies for FOX1, CRD1, and COX2b were generously provided by Dr. Sabeeha Merchant. The plasmids pDR196-GW and pDR196-GW-GFP were kindly provided by Dr. Dominique Loque.

Received April 16, 2010; accepted May 21, 2010; published May 24, 2010.



## LITERATURE CITED

- Abramoff MD, Magelhaes PJ, Ram SJ** (2004) Image processing with ImageJ. *Biophotonics Int* **11**: 36–42
- Allen MD, Kropat J, Merchant SS** (2008) Regulation and localization of isoforms of the aerobic oxidative cyclase in *Chlamydomonas reinhardtii*. *Photochem Photobiol* **84**: 1336–1342
- Arnon D** (1949) Copper enzymes in isolated chloroplasts: polyphenoloxidase in *Beta vulgaris*. *Plant Physiol* **24**: 1–15
- Breton A, Surdin-Kerjan Y** (1977) Sulfate uptake in *Saccharomyces cerevisiae*: biochemical and genetic study. *J Bacteriol* **132**: 224–232
- Chang CW, Moseley JL, Wykoff D, Grossman AR** (2005) The *LPB1* gene is important for acclimation of *Chlamydomonas reinhardtii* to phosphorus and sulfur deprivation. *Plant Physiol* **138**: 319–329
- Chen HC, Yokthongwattana K, Newton AJ, Melis A** (2003) SulP, a nuclear gene encoding a putative chloroplast-targeted sulfate permease in *Chlamydomonas reinhardtii*. *Planta* **218**: 98–106
- Cherest H, Davidian JC, Thomas D, Benes V, Ansoerg W, Surdin-Kerjan Y** (1997) Molecular characterization of two high affinity sulfate transporters in *Saccharomyces cerevisiae*. *Genetics* **145**: 627–637
- Colombo SL, Pollock SV, Eger KA, Godfrey AC, Adams JE, Mason CB, Moroney JV** (2002) Use of the bleomycin resistance gene to generate tagged insertional mutants of *Chlamydomonas reinhardtii* that require elevated CO<sub>2</sub> for optimal growth. *Funct Plant Biol* **29**: 231–241
- Davies JD, Grossman AR** (1998) Responses to deficiencies in macronutrients. In M Goldschmidt-Clermont, J-D Rochaix, S Merchant, eds, *The Molecular Biology of Chlamydomonas*. Kluwer Academic Publishers, Dordrecht, The Netherlands, pp 613–635
- Davies JP, Yildiz F, Grossman AR** (1994) Mutants of *Chlamydomonas* with aberrant responses to sulfur deprivation. *Plant Cell* **6**: 53–63
- Davies JP, Yildiz FH, Grossman A** (1996) Sac1, a putative regulator that is critical for survival of *Chlamydomonas reinhardtii* during sulfur deprivation. *EMBO J* **15**: 2150–2159
- DeWitt ND, dos Santos CF, Allen KE, Slayman CW** (1998) Phosphorylation region of the yeast plasma-membrane H<sup>+</sup>-ATPase: role in protein folding and biogenesis. *J Biol Chem* **273**: 21744–21751
- Eguez L, Chung YS, Kuchibhatla A, Paidhungat M, Garrett S** (2004) Yeast Mn<sup>2+</sup> transporter, Smf1p, is regulated by ubiquitin-dependent vacuolar protein sorting. *Genetics* **167**: 107–117
- Everett LA, Green ED** (1999) A family of mammalian anion transporters and their involvement in human genetic diseases. *Hum Mol Genet* **8**: 1883–1891
- Gonzalez E, Solano R, Rubio V, Leyva A, Paz-Ares J** (2005) PHOSPHATE TRANSPORTER TRAFFIC FACILITATOR1 is a plant-specific SEC12-related protein that enables the endoplasmic reticulum exit of a high-affinity phosphate transporter in *Arabidopsis*. *Plant Cell* **17**: 3500–3512
- Gonzalez-Ballester D** (2005) Genómica funcional de la señalización por amonio y nitrato, y caracterización de genes para el transporte de amonio en *Chlamydomonas*. PhD thesis. University of Cordoba, Cordoba, Spain
- Gonzalez-Ballester D, Casero D, Cokus S, Pellegrini M, Merchant SS, Grossman AR** (2010) RNA-seq analysis of sulfur-deprived *Chlamydomonas* cells reveals aspects of acclimation critical for cell survival. *Plant Cell* **22**: 2058–2084
- Gonzalez-Ballester D, Grossman AR** (2009) Sulfur: from acquisition to assimilation. In E Harris, D Stern, G Witman, eds, *The Chlamydomonas Sourcebook: Organellar and Metabolic Processes*. Elsevier, Amsterdam, pp 159–188
- Gonzalez-Ballester D, Pollock SV, Pootakham W, Grossman AR** (2008) The central role of a SNRK2 kinase in sulfur deprivation responses. *Plant Physiol* **147**: 216–227
- Grossman A, Takahashi H** (2001) Macronutrient utilization by photosynthetic eukaryotes and the fabric of interactions. *Annu Rev Plant Physiol Plant Mol Biol* **52**: 163–210
- Gyaneshwar P, Paliy O, McAuliffe J, Popham DL, Jordan MI, Kustu S** (2005) Sulfur and nitrogen limitation in *Escherichia coli* K-12: specific homeostatic responses. *J Bacteriol* **187**: 1074–1090
- Hawkesford MJ** (2003) Transporter gene families in plants: the sulphate transporter gene family—redundancy or specialization? *Physiol Plant* **117**: 155–163
- Herbik A, Bolling C, Buckhout TJ** (2002) The involvement of a multi-copper oxidase in iron uptake by the green algae *Chlamydomonas reinhardtii*. *Plant Physiol* **130**: 2039–2048
- Kataoka T, Hayashi N, Yamaya T, Takahashi H** (2004a) Root-to-shoot transport of sulfate in *Arabidopsis*: evidence for the role of SULTR3;5 as a component of low-affinity sulfate transport system in the root vasculature. *Plant Physiol* **136**: 4198–4204
- Kataoka T, Watanabe-Takahashi A, Hayashi N, Ohnishi M, Mimura T, Buchner P, Hawkesford MJ, Yamaya T, Takahashi H** (2004b) Vacuolar sulfate transporters are essential determinants controlling internal distribution of sulfate in *Arabidopsis*. *Plant Cell* **16**: 2693–2704
- Kawazoe R, Hwang S, Herrin DL** (2000) Requirement for cytoplasmic protein synthesis during circadian peaks of transcription of chloroplast-encoded genes in *Chlamydomonas*. *Plant Mol Biol* **44**: 699–709
- Ketter JS, Marzluf GA** (1988) Molecular cloning and analysis of the regulation of *cys-14<sup>+</sup>*, a structural gene of the sulfur regulatory circuit of *Neurospora crassa*. *Mol Cell Biol* **8**: 1504–1508
- Laudenbach DE, Grossman AR** (1991) Characterization and mutagenesis of sulfur-regulated genes in a cyanobacterium: evidence for function in sulfate transport. *J Bacteriol* **173**: 2739–2750
- Leustek T, Martin MN, Bick JA, Davies JP** (2000) Pathways and regulation of sulfur metabolism revealed through molecular and genetic studies. *Annu Rev Plant Physiol Plant Mol Biol* **51**: 141–165
- Lindberg P, Melis A** (2008) The chloroplast sulfate transport system in the green alga *Chlamydomonas reinhardtii*. *Planta* **228**: 951–961
- Maruyama-Nakashita A, Nakamura Y, Tohge T, Saito K, Takahashi H** (2006) *Arabidopsis* SLIM1 is a central transcriptional regulator of plant sulfur response and metabolism. *Plant Cell* **18**: 3235–3251
- Melis A, Chen HC** (2005) Chloroplast sulfate transport in green algae: genes, proteins and effects. *Planta* **86**: 299–307
- Merchant SS, Prochnik SE, Vallon O, Harris EH, Karpowicz SJ, Witman GB, Terry A, Salamov A, Fritz-Laylin LK, Marechal-Drouard L, et al** (2007) The *Chlamydomonas* genome reveals the evolution of key animal and plant functions. *Science* **318**: 245–250
- Moseley JL, Gonzalez-Ballester D, Pootakham W, Bailey S, Grossman AR** (2009) Genetic interactions between regulators of *Chlamydomonas* phosphorus and sulfur deprivation responses. *Genetics* **181**: 889–905
- Navarro FJ, Martín Y, Siverio JM** (2008) Phosphorylation of the yeast nitrate transporter Ynt1 is essential for delivery to the plasma membrane during nitrogen limitation. *J Biol Chem* **283**: 31208–31217
- Norling B, Nurani G, Franzén LG** (1996) Characterisation of the H<sup>+</sup>-ATPase in plasma membranes isolated from the green alga *Chlamydomonas reinhardtii*. *Physiol Plant* **97**: 445–453
- Page MD, Kropat J, Hamel PP, Merchant SS** (2009) Two *Chlamydomonas* CTR copper transporters with a novel Cys-Met motif are localized to the plasma membrane and function in copper assimilation. *Plant Cell* **21**: 928–943
- Pollock SV, Colombo SL, Prout DL Jr, Godfrey AC, Moroney JV** (2003) Rubisco activase is required for optimal photosynthesis in the green alga *Chlamydomonas reinhardtii* in a low-CO<sub>2</sub> atmosphere. *Plant Physiol* **133**: 1854–1861
- Pollock SV, Pootakham W, Shibagaki N, Moseley JL, Grossman AR** (2005) Insights into the acclimation of *Chlamydomonas reinhardtii* to sulfur deprivation. *Photosynth Res* **86**: 475–489
- Rouached H, Berthomieu P, El Kassis E, Cathala N, Catherinot V, Labesse G, Davidian JC, Fourcroy P** (2005) Structural and functional analysis of the C-terminal STAS (sulfate transporter and anti-sigma antagonist) domain of the *Arabidopsis thaliana* sulfate transporter SULTR1.2. *J Biol Chem* **280**: 15976–15983
- Sambrook J, Fritsch EF, Maniatis T** (1989) *Molecular Cloning: A Laboratory Manual*. Cold Spring Harbor Laboratory Press, Cold Spring Harbor, NY
- Shibagaki N, Grossman AR** (2004) Probing the function of STAS domains of the *Arabidopsis* sulfate transporters. *J Biol Chem* **279**: 30791–30799
- Shibagaki N, Grossman AR** (2006) The role of the STAS domain in the function and biogenesis of a sulfate transporter as probed by random mutagenesis. *J Biol Chem* **281**: 22964–22973
- Shibagaki N, Grossman AR** (2008) The state of sulfur metabolism in algae: from ecology to genomics. In R Hell, C Dahl, D Knaff, T Leustek, eds, *Advances in Photosynthesis and Respiration: Sulfur Metabolism in Photoautotrophic Organisms*. Springer, Dordrecht, The Netherlands, pp 231–267
- Shibagaki N, Grossman AR** (2010) The binding of cysteine synthase to the STAS domain of sulfate transporter and its regulatory consequences. *J Biol Chem* (in press)
- Shibagaki N, Rose A, McDermott JP, Fujiwara T, Hayashi H, Yoneyama T, Davies JP** (2002) Selenate-resistant mutants of *Arabidopsis thaliana*



- identify Sultr1;2, a sulfate transporter required for efficient transport of sulfate into roots. *Plant J* **29**: 475–486
- Shimogawara K, Fujiwara S, Grossman A, Usuda H** (1998) High-efficiency transformation of *Chlamydomonas reinhardtii* by electroporation. *Genetics* **148**: 1821–1828
- Sizova I, Fuhrmann M, Hegemann P** (2001) A *Streptomyces rimosus aphVIII* gene coding for a new type phosphotransferase provides stable antibiotic resistance to *Chlamydomonas reinhardtii*. *Gene* **277**: 221–229
- Smalle J, Vierstra RD** (2004) The ubiquitin 26S proteasome proteolytic pathway. *Annu Rev Plant Biol* **55**: 555–590
- Takahashi H, Braby CE, Grossman AR** (2001) Sulfur economy and cell wall biosynthesis during sulfur limitation of *Chlamydomonas reinhardtii*. *Plant Physiol* **127**: 665–673
- Takahashi H, Watanabe-Takahashi A, Smith FW, Blake-Kalff M, Hawkesford MJ, Saito K** (2000) The roles of three functional sulphate transporters involved in uptake and translocation of sulphate in *Arabidopsis thaliana*. *Plant J* **23**: 171–182
- Takahashi H, Yamazaki M, Sasakura N, Watanabe A, Leustek T, Engler JA, Engler G, Van Montagu M, Saito K** (1997) Regulation of sulfur assimilation in higher plants: a sulfate transporter induced in sulfate-starved roots plays a central role in *Arabidopsis thaliana*. *Proc Natl Acad Sci USA* **94**: 11102–11107
- Tejada-Jiménez M, Llamas A, Sanz-Luque E, Galvan A, Fernandez E** (2007) A high-affinity molybdate transporter in eukaryotes. *Proc Natl Acad Sci USA* **104**: 20126–20130
- Wolf DH** (2004) From lysosome to proteasome: the power of yeast in the dissection of proteinase function in cellular regulation and waste disposal. *Cell Mol Life Sci* **61**: 1601–1614
- Yildiz FH, Davies JP, Grossman AR** (1994) Characterization of sulfate transport in *Chlamydomonas reinhardtii* during sulfur-limited and sulfur-sufficient growth. *Plant Physiol* **104**: 981–987
- Yoshimoto N, Takahashi H, Smith FW, Yamaya T, Saito K** (2002) Two distinct high-affinity sulfate transporters with different inducibilities mediate uptake of sulfate in *Arabidopsis* roots. *Plant J* **29**: 465–473
- Zhang Z, Shrager J, Jain M, Chang CW, Vallon O, Grossman AR** (2004) Insights into the survival of *Chlamydomonas reinhardtii* during sulfur starvation based on microarray analysis of gene expression. *Eukaryot Cell* **3**: 1331–1348